JOURNAL OF GEOPHYSICAL RESEARCH, VOL. 107, NO. D20, 8082, doi:10.1029/2001JD000380, 2002

# Contrasting convective regimes over the Amazon: Implications for cloud electrification

E. Williams,[1] D. Rosenfeld,[2] N. Madden,[1] J. Gerlach,[3] N. Gears,[3] L. Atkinson,[3] N. Dunnemann,[3] G. Frostrom,[3] M. Antonio,[4] B. Biazon,[4] R. Camargo,[4] H. Franca,[4] A. Gomes,[4] M. Lima,[4] R. Machado,[4] S. Manhaes,[4] L. Nachtigall,[4] H. Piva,[4] W. Quintiliano,[4] L. Machado,[5] P. Artaxo,[6] G. Roberts,[7] N. Renno,[8] R. Blakeslee,[9] J. Bailey,[9] D. Boccippio,[9] A. Betts,[10] D. Wolff,[11] B. Roy,[11] J. Halverson,[11] T. Rickenbach,[11] J. Fuentes,[12] and E. Avelino[13]

Received 16 January 2001; revised 20 August 2001; accepted 10 December 2001; published 10 October 2002.

[1] Four distinct meteorological regimes in the Amazon basin have been examined to distinguish the contributions from boundary layer aerosol and convective available potential energy (CAPE) to continental cloud structure and electrification. The lack of distinction in the electrical parameters (peak flash rate, lightning yield per unit rainfall) between aerosol-rich October and aerosol-poor November in the premonsoon regime casts doubt on a primary role for the aerosol in enhancing cloud electrification. Evidence for a substantial role for the aerosol in suppressing warm rain coalescence is identified in the most highly polluted period in early October. The electrical activity in this stage is qualitatively peculiar. During the easterly and westerly wind regimes of the wet season, the lightning yield per unit of rainfall is positively correlated with the aerosol concentration, but the electrical parameters are also correlated with CAPE, with a similar degree of scatter. Here cause and effect are difficult to establish with available observations. This ambiguity extends to the ''green ocean'' westerly regime, a distinctly maritime regime over a major continent with minimum aerosol concentration, minimum CAPE, and little if any lightning. *INDEX TERMS:* 0305 Atmospheric Composition and Structure: Aerosols and particles (0345, 4801); 3304 Meteorology and Atmospheric Dynamics: Atmospheric electricity; 3314 Meteorology and Atmospheric Dynamics: Convective processes; 3324 Meteorology and Atmospheric Dynamics: Lightning; 3374 Meteorology and Atmospheric Dynamics: Tropical meteorology; *KEYWORDS:* lightning, convention, aerosol, regimes, radar, precipitation

**Citation:** Williams, E., et al., Contrasting convective regimes over the Amazon: Implications for cloud electrification, *J. Geophys. Res.*, *107*(D20), 8082, doi:10.1029/2001JD000380, 2002.

## 1. Introduction

### 1.1. Maritime Versus Continental Convective Regimes

[2] Cloud physicists have traditionally designated clouds as ''maritime'' and ''continental'' based on their microstructure, where maritime clouds contain small concentrations (about 50 to 100 $cm^{-3}$) of large droplets and continental clouds contain tenfold-larger concentrations of smaller droplets. The difference has been linked to the large difference in the concentrations of cloud condensation nuclei (CCN) over land and ocean (see Figure 1). These differences in cloud droplet sizes over land and ocean were translated to a large difference in the ''colloidal stability'' of the clouds, as defined by *Squires* [1958], who coined the terms maritime and continental clouds. Maritime clouds precipitate easily by warm processes, whereas coalescence is often suppressed in continental clouds, which often have to grow to supercooled levels to precipitate by ''cold'' processes, i.e., involving the ice phase. This definition of the convective clouds remained merely a microphysical one, until the observations of lightning from space became available, revealing a dramatic contrast between the lightning over land and ocean [*Orville and Henderson*, 1986]. That gave a whole new meaning to the determination of maritime and continental clouds and triggered a series of investigations trying to understand the causes for the contrast between the convective regimes over the tropical lands

[1]Massachusetts Institute of Technology, Cambridge, Massachussets, USA.
[2]Hebrew University, Jerusalem, Israel.
[3]NASA Wallops Island Flight Facility, Wallops Island, Virginia, USA.
[4]University of the State of Sao Paulo, IPMET, Bauru, Brazil.
[5]Centro Tecnico Aeroespacial, Sao Jose dos Campos, Sao Paulo, Brazil.
[6]University of Sao Paulo, Sao Paulo, Brazil.
[7]Max Planck Institute for Chemistry, Mainz, Germany.
[8]University of Arizona, Tucson, Arizona, USA.
[9]NASA Marshall Space Flight Center, Huntsville, Alabama, USA.
[10]Atmospheric Research, Pittsford, Vermont, USA.
[11]NASA Goddard Space Flight Center, Greenbelt, Maryland, USA.
[12]University of Virginia, Charlottesville, Virginia, USA.
[13]Embratel, Porto Velho, Rondonia, Brazil.


0148-0227/02/2001JD000380$09.00

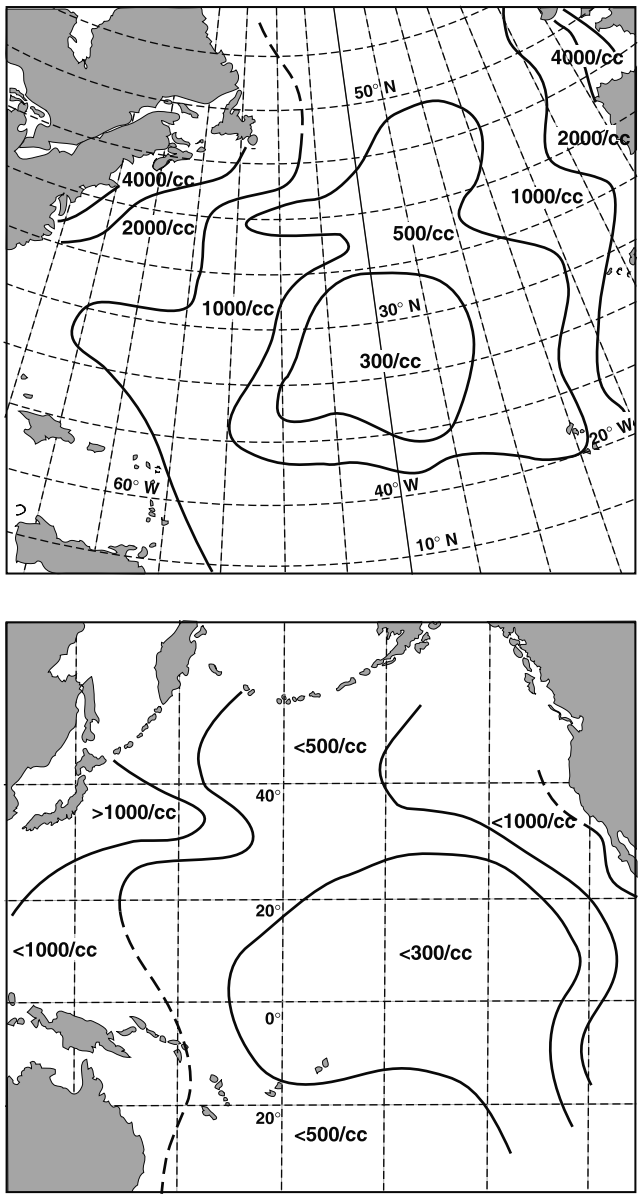


**Figure 1.** Maps of condensation nuclei (CN) for the Atlantic and Pacific Oceans [after *Hogan*, 1977]. The concentration of cloud condensation nuclei (CCN) at 1% supersaturation is estimated to be about half these values (A. Hogan, personal communication, December 2000).

and oceans [*Williams et al.*, 1992; *Rutledge et al.*, 1992; *Zipser*, 1994; *Lucas et al.*, 1994; *DeMott and Rutledge*, 1998], and became a major focus in the 1999 Brazil field experiment to be discussed here [*Cifelli et al.*, 2002; *Halverson et al.*, 2002; *Petersen et al.*, 2002]. In the search for explanations, some notable differences have been documented between maritime and continental convective clouds:

1. There was distinctly less supercooled water limited to higher temperatures in the tropical maritime compared with the continental clouds [*Zipser and LeMone*, 1980; *Black and Hallett*, 1986].

2. The updraft velocities in maritime clouds were characteristically limited to below the terminal fall velocity of the raindrops, whereas no such maximum for the updraft was noted in continental convection [*Zipser and LeMone*, 1980; *Jorgensen and LeMone*, 1989; *Zipser and Lutz*, 1994].

3. The vertical profiles of radar reflectivity in the mixed phase region are substantially stronger in continental than in maritime clouds [*Williams et al.*, 1992; *Rutledge et al.*, 1992; *Zipser*, 1994; *Zipser and Lutz*, 1994].

[3] In the next section we will review how both microphysical (CCN and cloud droplet size distribution) and dynamical (updraft velocity) cloud properties are capable of influencing precipitation processes, convective development, and cloud electrification.

### 1.2. Links Between Cloud Dynamics, Microphysics, and Electrification

[4] In spite of the usual association of deep cumulonimbus clouds with thunderstorms, much of the deep convection in the tropics is not associated with thunderstorms. The electrification of clouds is caused by collisions of graupel and ice crystals in a supercooled cloud [*Reynolds et al.*, 1957; *Takahashi*, 1978; *Saunders et al.*, 1991]. The supercooled water supply is maintained by the updraft. The separation of charge occurs by gravity-driven differential particle motions. The rate of electrification depends on the rate of particle collisions per unit cloud volume. Laboratory experiments show only a slight dependence of the charging rate on the amount of supercooled water. They rather suggest that the charging is switched on with the existence of the supercooled water in a cloud in which collisions between graupel and ice crystals occur.

[5] Clouds devoid of lightning must lack either supercooled water or ice. In deep tropical convection, lack of ice is not a probable cause [*Churchill and Houze*, 1984] except for extremely continental clouds [*Rosenfeld and Woodley*, 2000]. Therefore lack of supercooled water appears to be the direct cause for deep maritime convective clouds without lightning. This lack of lightning in maritime tropical clouds has been associated with lack of supercooled water, which in turn has been attributed mainly to the weak midlevel updrafts characteristic of these clouds. This situation is conducive to commonly described conditions in the supercooled levels in equatorial tropical convective clouds, as having low supercooled liquid water content, high concentrations of small ice particles (<0.5 mm), and near absence of large ice particles (>1 mm) [*Black and Hallett*, 1986; *Zipser and LeMone*, 1980; *Lucas et al.*, 1994]. The scarcity of large ice particles and supercooled water above the 0°C isotherm provides little support for electrical charging and returns only weak radar echoes. Both weak updrafts and rapid coalescence in maritime clouds can in principle result in rapid depletion of their cloud water while growing. When combined with the lack of large graupel, these clouds are missing two key ingredients thought to produce charge separation leading to lightning. *Zipser and Lutz* [1994] wrote as follows: "An updraft with diameter 2–3 km, average speed 6–7 m $s^{-1}$, and maximum speed 10–12 m $s^{-1}$ (Figure 3) would be capable of balancing raindrops with diameters in the 1.5–2.5 mm range. This is considerably stronger than the 10th percentile updraft over tropical oceans. We suggest that updrafts near this strength are near a bifurcation point, such that cloud

microphysical properties in the cell are very different below and above this threshold.''

[6] The differences in updraft strength above land and ocean surfaces has long been identified as the cause for differences in the cloud microphysical and electrical properties. The longstanding traditional explanation for the land-ocean contrast is simply that land surfaces respond more strongly to solar radiation, and the overlying boundary layer air becomes more strongly buoyant in relation to its surroundings. The larger cloud buoyancy leads to stronger continental updrafts, which in turn invigorate ice microphysics favorable to charge separation and lightning. This interpretation has been invoked to explain the dramatic contrast in lightning activity between break period (''continental'') and monsoonal (''maritime'') convection in northern Australia [*Rutledge et al.*, 1992; *Williams et al.*, 1992]. Various published hypotheses differ on the microphysical details, but the vertically integrated cloud buoyancy (otherwise known as convective available potential energy (CAPE)) and the updraft speed are common parameters. *Williams et al.* [1992] and *Rutledge et al.* [1992] suggested that ice particle growth by riming is nonlinearly dependent on updraft speed. *Zipser and Lutz* [1994] suggested that larger updraft speeds would enable delivery of supercooled raindrops to the mixed phase region, where they could participate in charge separation. In their emphasis on large precipitation particles, hypotheses in this class predict substantial land-ocean contrast in radar reflectivity within the mixed phase region, the apparent seat of lightning activity. This traditional explanation linking boundary layer temperature, cloud buoyancy, and ice microphysics also forms the basis for ideas that global lightning activity, and hence the global electrical circuit, will show responsiveness to changes in surface air temperature [*Williams*, 1992, 1994, 1999; *Price*, 1993; *Markson and Lane-Smith*, 1994; *Fullekrug and Fraser-Smith*, 1997; *Reeve and Toumi*, 1999; *Watkins et al.*, 2001].

[7] The main goal of this study is to distinguish the roles of aerosol and CAPE on the regime-to-regime differences in electrification. The goal has been challenging because many of the available observables (radar initial echo height, warm rain coalescence, the rainout process, and electrical activity) are similarly influenced by aerosol and updraft. The findings of this study tend to support the traditional CAPE-based explanation for the lightning-active premonsoon period in Brazil. A prominent role for aerosol in suppressing warm rain coalescence is identified in the highly polluted period in the early premonsoon. The role of the aerosol on cloud vertical development and electrification during the wet season in which a distinct maritime-like regime is identified and called the ''green ocean,'' is least well defined, and deserves further study.

### 1.3. The Aerosol Hypothesis

[8] The present study tests a distinctly different hypothesis for the contrast in lightning activity in continental and maritime clouds. This explanation, as proposed by D. Rosenfeld for this study, is based on another well-established contrast between continental and maritime boundary layers: the aerosol concentration. Figure 1 shows maps of condensation nuclei concentrations for the ''blue'' oceans, Atlantic and Pacific [*Hogan*, 1977]. The boundary layer air far from continents is very clean, with values of the order of 300 $cm^{-3}$, but becomes increasingly polluted near the ocean fringes and into the continents. The continental aerosol concentration is decidedly greater but extraordinarily variable, which is one of several reasons that global maps of condensation nuclei do not exist. The mean land-ocean contrast is probably of the order of 5–20. The influence of this strong aerosol contrast on the behavior of the electrical conductivity of the fair weather boundary layer and its contrast with that of the free troposphere is also well established [*Sagalyn and Faucher*, 1954; *Sagalyn*, 1958].

[9] The aerosol hypothesis for the land-ocean lightning contrast is illustrated in Figure 2. In contrast with the dominant role of large particles in the traditional hypothesis, this idea focuses on the behavior of the smaller cloud droplets. Air drawn from the clean (polluted) boundary layer air will contain a small (large) number of large (small) droplets. Active coalescence and rainout of the cloud prevail in the warm portion of the maritime cloud, leading to the depletion of liquid water from the colder mixed phase region. A dominance of diffusional droplet growth and suppressed coalescence prevail in the continental CCN-rich clouds, preventing rainout and allowing liquid water to ascend to the mixed phase region where it plays a dual role. First, it can contribute to cloud buoyancy and the updraft strength by the latent heat of freezing. Second, it can contribute to the growth of graupel particles and catalyze the process of charge separation by ice particle collisions.

[10] In clouds with very large concentrations of small CCN the formation of the ice phase can be delayed to very high altitudes and low temperatures [*Rosenfeld and Lensky*, 1998; *Rosenfeld*, 2000; *Rosenfeld and Woodley*, 2002; *Khain et al.*, 2001]. The delay in the ice formation to above the −20°C isotherm is likely to deprive the lower part of the mixed phase region of a key ingredient for charge separation in a temperature range where it is most potent [*Takahashi*, 1978], and thereby addition of aerosols beyond a certain ''optimum'' may not enhance any more lightning, and may even decrease it with respect to that ''optimum.''

[11] The contrast in updrafts between land and ocean convective clouds is well established as a major cause for the differences between the land and ocean lightning activity, and this result is reinforced in this study. An unresolved question is the cause for this fundamental difference in updrafts, but attempting to resolve that question is beyond the scope of this study. However, the aerosol contrast between land and ocean is also well established [Figure 1], so that it can provide an additional (not alternative) explanation for the pronounced differences in lightning between land and ocean [*Orville and Henderson*, 1986; *Christian et al.*, 1999].

[12] Rather than visit different regions of land and ocean to examine these questions, the chosen strategy has been to study convection at a single location in Rondonia, Brazil, where the seasonal variation of aerosol concentration is similar to the land-ocean aerosol contrast shown in Figure 1. Measurements in Brazil designed to test the qualitative ideas illustrated in Figure 2 for both the liquid and solid phase of water include radar cross sections of the vertical structure in mature stages, electrical measurements of lightning peak flash rates, radar measurements of total daily for comparison with daily lightning totals, and advanced very high reso-

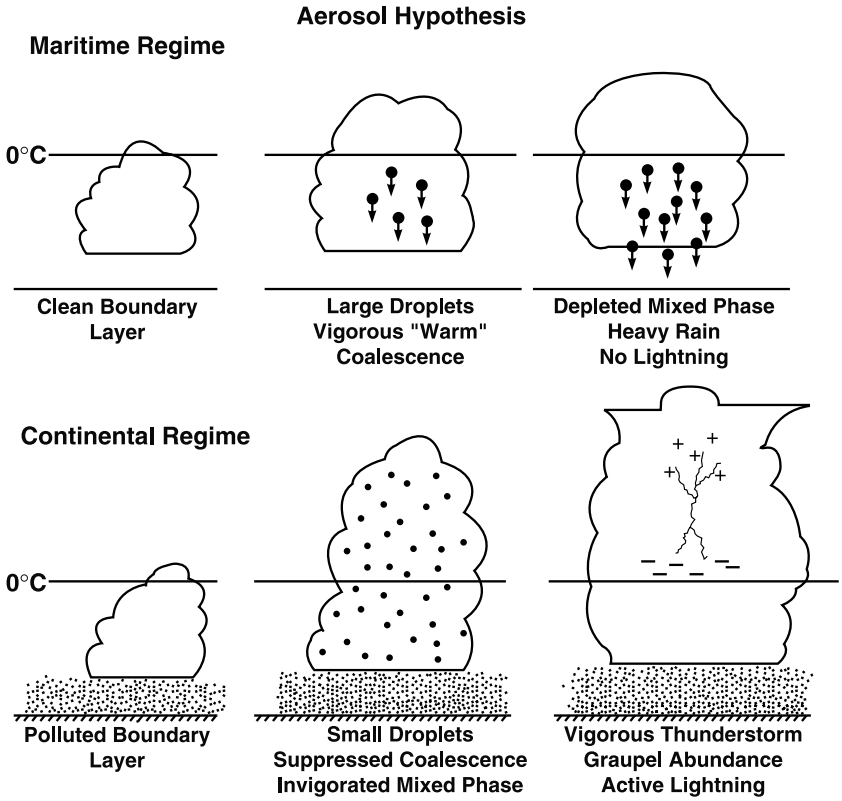


**Figure 2.** Illustration of the aerosol hypothesis for control of cloud precipitation and electrification.

lution radiometer (AVHRR) satellite measurements of the evolution of cloud particle size and glaciation.

## 2. Meteorological Regimes

[13] The distinction in physical behavior between maritime and continental convection is a key aspect of this study. The convective regime at specific locations in tropical South America can vary from polluted continental to clean maritime depending primarily on the location of the Intertropical Convergence Zone (ITCZ), which, in turn, depends on the season. The continental ITCZ in South America is rarely longitudinally confined, however, and the interpretation of regime changes in terms of the latitudinal position of the ITCZ is more complicated here than in tropical Australia [*Williams et al.*, 1992; *Rutledge et al.*, 1992]. Studies by *Rickenbach et al.* [2002] and *Petersen et al.* [2002] have shown that the penetration of frontal circulations from the extratropics and the equatorial penetration of the South Atlantic Convergence Zone (SACZ) are both influential in changing the zonal wind direction from easterly to westerly. These two predominant wind directions conveniently define two regimes within the Rondonian wet season [*Rickenbach et al.*, 2002]. The convection in the easterly regime is typefied by strong updrafts, large concentrations of aerosols, and abundant lightning. The westerly regime is typefied by oceanic like clouds, clean air, weak updrafts, strong coalescence, and scarcity of lightning. The vast Amazon rain forest can be viewed as a ''green ocean'' beneath this westerly regime.

[14] Prior to the onset of the regular wet season, with its alternating periods of easterly and westerly wind, Rondonia experiences a ''premonsoon'' phase, characterized by continental conditions which can be more extreme than the easterly regime. Large-scale subsidence from the distant ITCZ is strong, solar insolation is maximum because of the latitudinal position of the Sun, rainfall is relatively infrequent, the surface Bowen ratio is large [*Betts et al.*, 2002], and biomass burning with abundant aerosol production is prevalent. As the rainfall increases with the approach of the ITCZ, the atmosphere gradually clears.

[15] The specific regimes examined in this study and their respective time periods are summarized in Table 1.

[16] Figure 3 shows the rainfall climatology for Ouro Preto, Rondonia (the location of the field experiment as shown in Figure 4) based on a 12-year record (1982–1994), from July to June. The wet season portion of this study took place during January to March, when the integrated rainfall is maximum, and hence the period of highest probability for the ITCZ to lie over the Ouro Preto region. The opposite extreme, July, shows the minimum rainfall (8.3 mm) and marks the middle of the dry season when Ouro Preto is in a zone of subsidence from the ITCZ to the north. The

**Table 1.** Meteorological Regimes in Rondonia, Brazil (1999)

| Regime Name | Duration |
|---|---|
| Wet season westerly | 10 Jan. (0000 UT) to 19 Jan. (0000 UT) |
| wind regime | 27 Jan. (0000 UT) to 8 Feb. (0000 UT) |
| (the ''green ocean'') | 22 Feb. (0000 UT) to 8 March (0000 UT) |
| Wet season easterly | 19 Jan. (0000 UT) to 27 Jan. (0000 UT) |
| wind regime | 8 Feb. (0000 UT) to 22 Feb. (0000 UT) |
| Polluted premonsoon regime | 10 Oct. (0000 UT) to 28 Oct. (0000 UT) |
| ''Clean'' premonsoon regime | 29 Oct. (0000 UT) to 30 Nov. (0000 UT) |

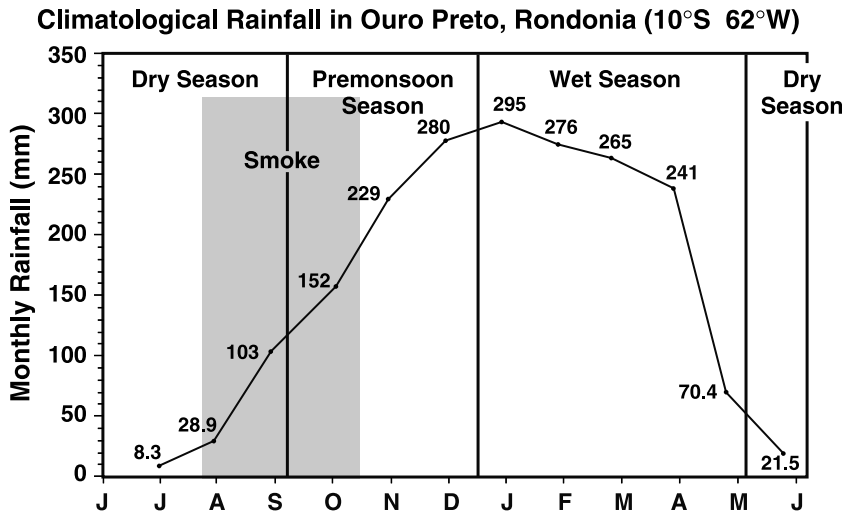


**Figure 3.** Seasonal rainfall climatology [after *Scerne et al.*, 1996] for Ouro Preto, Rondonia, Brazil, including the identification of prominent meteorological regimes.

premonsoon period (September–December) is clearly seen in the rainfall record as the interval during which the continental ITCZ is migrating southward and rainfall is increasing. The premonsoon field study began in October for which the mean climatological rainfall (152 mm) is roughly half its value in the peak of the wet season (295 mm).

## 3. Methodology for Regime Characterization

### 3.1. Radar Measurements

[17] The NASA Tropical Ocean–Global Atmosphere (TOGA) C band Doppler radar was installed in December 1998 on a hilltop (Abracos Hill) on the Fazenda Boa Vista (10°46′S, 62°22′W) near Ouro Preto, Rondonia (Figure 4). The radar was operated around the clock beginning in early January, on a 10-min update with full volume scans. These scan sequences were coordinated with those of the SPOL radar, 62 km to the southeast. Radar range-height indicator (RHI) scans were interspersed between the 10-min volume scans as time and interest warranted. The TOGA radar operation ceased in March 1999 for the duration of the dry season but was resumed in early October 1999. This second operation ran from early morning until late evening, depending on the convective activity. Radar operators

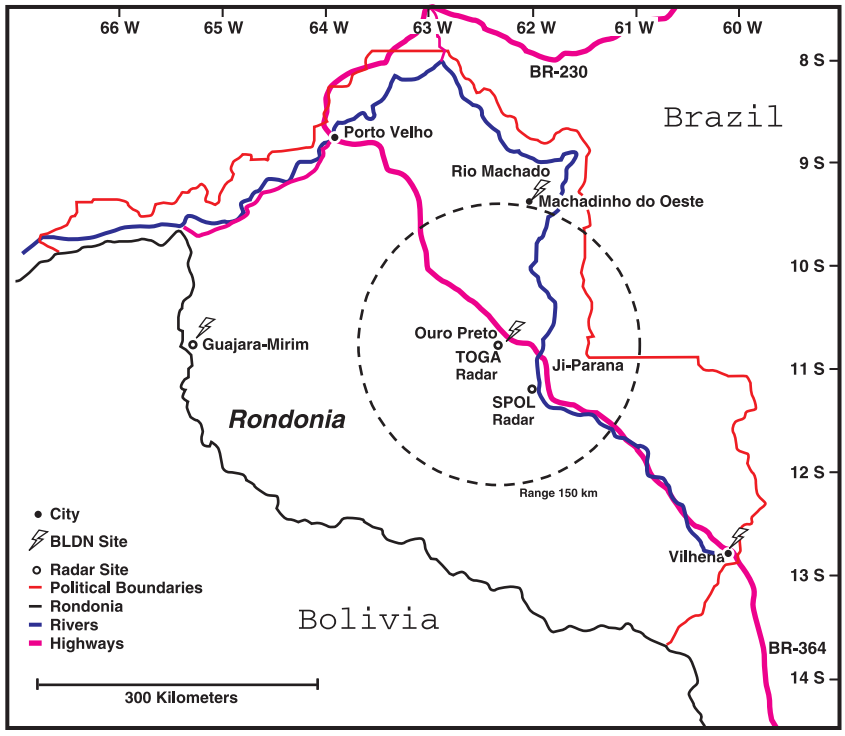


**Figure 4.** Map of Rondonia, Brazil, showing TOGA and SPOL radar locations and the four stations of the Brazil Lightning Detection Network (BLDN). The river stage measurements were obtained near the intersection of the Rio Machado and the main highway (BR 364).

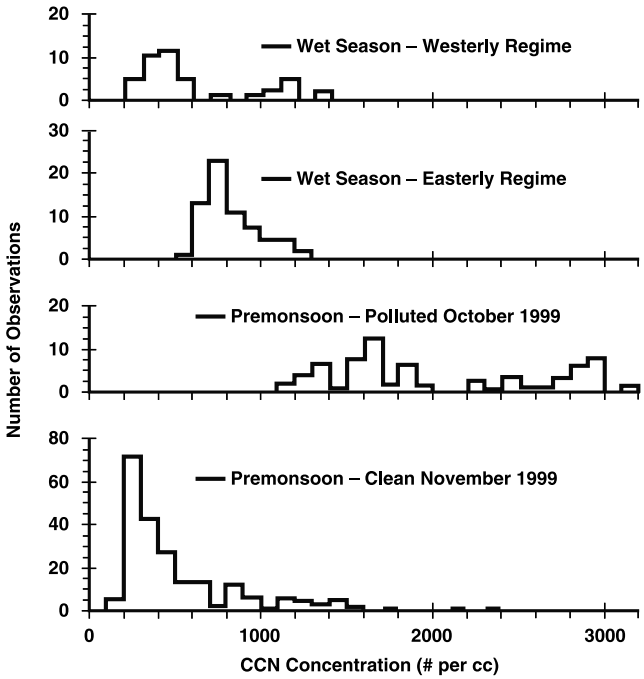


**Figure 5.** Summary of cloud condensation nuclei concentrations measured at a supersaturation of 1% in different meteorological regimes in Rondonia, Brazil, during 1999.

followed the development of reflectivity in the real time volume scans. Numerous RHI scans at preselected azimuths were then used to document the vertical development of the most vigorous convective cells. These RHI scans will be presented later for selected case study days.

[18] For purposes of characterizing the rainfall production regime to regime, TOGA radar observations were used to obtain daily rainfall estimates within a circular area with 150-km radius. Reflectivity observations from the lowest-elevation plan position indicator (PPI) scans were converted to rainfall rate (and ultimately to mass flux) by using the *Z-R* relation

$$Z = 241\ R^{1.54}$$

where $R$ is expressed in millimeters per hour and $Z$ is in units of $mm^6/m^3$. The resulting mass fluxes were then integrated over area and over all 10-min volume scan intervals to obtain a daily rainfall mass in kilograms.

### 3.2. Boundary Layer Aerosol Measurements

[19] Measurements of cloud condensation nuclei were carried out in Brazil with an M1 CCN counter, a parallel plate diffusion chamber with optical particle counter, designed by Sean Twomey and manufactured by DH Associates of Tucson, Arizona [*Phillipin and Betterton*, 1997]. The same instrument had been used by Battelle Laboratories in an aircraft study of the Kuwait oil fire plumes in 1991 [*Busness et al.*, 1992].

[20] The CCN measurements in Brazil were supplemented with condensation nuclei measurements with a TSI condensation nuclei counter (model TSI 3010 CPC, TSI Inc., St. Paul, Minnesota) using butanol as the nucleated vapor. Operated at very large supersaturations, this instrument is expected to record all aerosol particles down to 10-nm size. In practice, this device produced total concentrations, which are typically 1.5–4 times the values recorded by the CCN counter near 1% supersaturation. Occasionally, in highly polluted conditions associated with boundary layer smoke, the CN/CCN ratios exceeded 10 to 1.

[21] Representative samples of CCN concentration (at 1% supersaturation) in the four regimes summarized in Table 1 are shown in Figure 5. The cleanest air during the field program was found in the green ocean westerly regime and the latter portion of the premonsoon, when values of less than 200 $cm^{-3}$ were occasionally observed, most frequently in the presence of widespread rainfall. The median CCN value in the westerly phase is 400 $cm^{-3}$, which is similar to the mean value for the maritime phase of convection in Florida [*Hudson and Yum*, 2001]. Their similarity to true maritime levels is verified by comparison with the CN maps in Figure 1, where values less than 300 $cm^{-3}$ (roughly 150 CCN $cm^{-3}$) are documented for mid-ocean. Similarly, ocean-like levels for CCN concentration over the Amazon region have been documented by *Roberts et al.* [2001].

[22] The easterly regime is decidedly more polluted, consistent with the more continental nature of this convection. The contrast with the green ocean levels is still only a factor of 2 in the mean, and this regime is therefore still cleaner than typical continental conditions at midlatitudes.

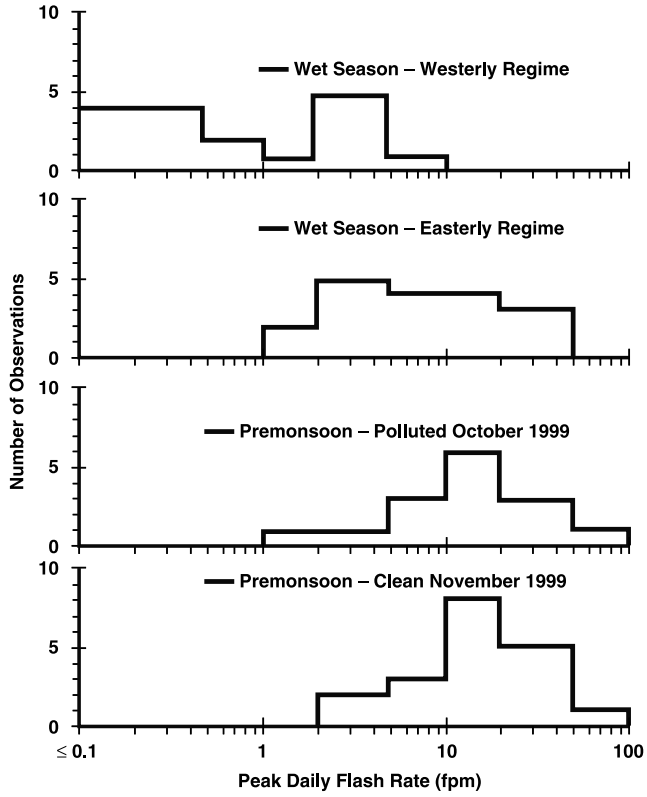


**Figure 6.** Summary of peak daily flash rate with the field change antenna at the TOGA radar site, in different meteorological regimes in Rondonia, Brazil, during 1999.

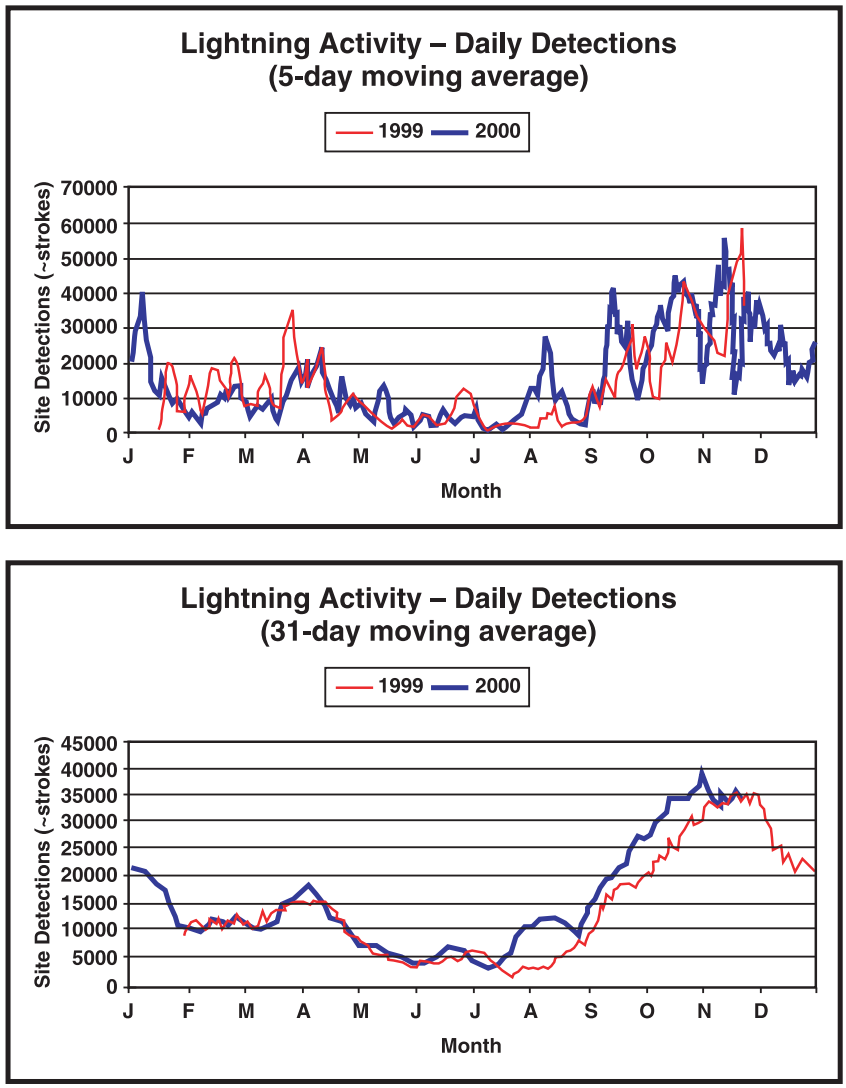


**Figure 7.** BLDN network-integrated counts of cloud-to-ground flashes from February 1999 to December 2000. A one-month running mean filter has been applied to the daily record to produce these curves.

[23] The most strongly polluted conditions, with CCN concentrations exceeding 3000 $cm^{-3}$ in daily means, occurred in the transition from the dry to the wet season during September and October. Scattered fires throughout Rondonia and the neighboring state of Mato Grosso set up a widespread pall with pronounced degradation of visibility in early October, when local CN concentrations frequently exceeded 30,000 $cm^{-3}$, beyond the operating range of the CCN counter. The label "supercontinental" is most appropriate for this regime.

### 3.3. Lightning Observations and Lightning Yield per Unit Rainfall

[24] Quantitative measurements of lightning activity are essential in this study. Two sources of lightning information were available in the Brazil field program.

[25] Total lightning activity within approximately 30–40 km of the TOGA radar was measured with field change antennae equipped with flat plate electrodes identical to instruments used earlier in Australia [*Williams et al.*, 1992]. One such instrument was deployed on a vertical mast for maximum sensitivity and another instrument was flush-mounted in the Earth on a flat portion of Abracos Hill for calibrated measurements of the electric field change. Distinct abrupt field changes associated with both intracloud and cloud-to-ground lightning flashes were counted to provide the total flash rate on a continuous basis. The maximum range of detection is limited by the rapid ($D^{-3}$) falloff of a dipole field with distance and by the screening effect of the conductive lower ionosphere. Daily digital records were searched for the maximum flash rate of the day as one measure of convective vigor.

[26] Figure 6 shows regime comparisons of peak flash rate, using all days available for each of four regimes. Peak flash rate is an important distinguishing characteristic in this study for different regimes. (A logarithmic scale is used here in contrast to the linear scale for the CCN regime comparison in Figure 5.) The green ocean westerly regime is clearly characterized by low flash rates or by no lightning at all. No flash rate greater than 10 flashes per minute (fpm)

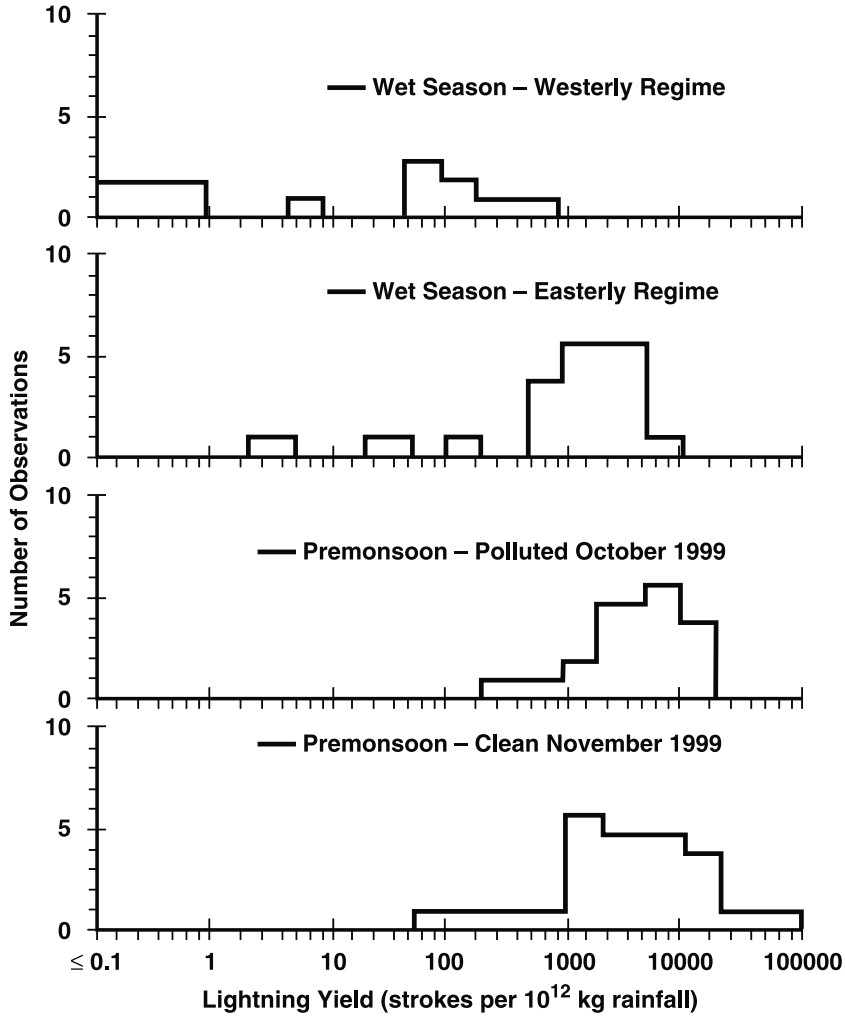


**Figure 8.** Summary of daily lightning yield (strokes per $10^{12}$ kg rainfall) based on lightning strokes recorded with the BLDN and rainfall with the TOGA radar, in different meteorological regimes in Rondonia, Brazil, during 1999.

is observed. The mean flash rate in the more continental easterly and premonsoon regimes is larger by an order of magnitude. The largest flash rates of all (occasionally exceeding 60 fpm) were observed during the preomonsoon phase "far" from the green ocean, a behavior consistent with earlier findings in Australia [*Williams et al.*, 1992; *Rutledge et al.*, 1992].

[27] A more representative measurement of lightning activity on the radar surveillance scale (Figure 4) was made possible by the Brazil Lightning Detection Network (BLDN) installed by NASA Marshall Space Flight Center in collaboration with INMET (the Brazilian national meteorological agency) in late 1998. Sensors for the detection of cloud-to-ground lightning flashes, manufactured by Global Atmospherics, Inc. (Tucson, Arizona), were deployed at four sites within the state of Rondonia, as shown in Figure 4. The multistation observations were used to locate ground flashes and record their peak return stroke currents, polarity, and stroke multiplicity. The approximate radius of detection for this network is 500 km. Data acquisition began in February 1999 and is continuous to present. Figure 7 shows this entire 2-year record of ground flash detections over the network. The wet season interval when green ocean rainfall is most prevalent (December–March; see Figure 3) is consistently a period of reduced lightning activity relative to the premonsoon, even when the more lightning-active easterly regime is not removed from the wet season record. (A more extensive BLDN comparison of the easterly and westerly regimes in Brazil may be found in the work of *Petersen et al.* [2002].

[28] The seasonal lightning record (Figure 7) and the seasonal rainfall record (Figure 3) are distinctly different. The rainfall record is dominated by a strong annual signal, in phase with the green ocean behavior. The lightning record is characterized more strongly by a semiannual component, with maxima in both transition periods (i.e., both the onset and the recession of the wet season). The characteristic semiannual signal from lightning activity in near-equatorial continental zones has been discussed previously [*Williams*, 1994; *Satori and Zieger*, 1996; *Fullekrug and Fraser-Smith*, 1997; *Williams*, 1999].

[29] An important additional parameter for characterizing the convection regime to regime and testing the relative roles of updraft and CCN on the electrification was obtained

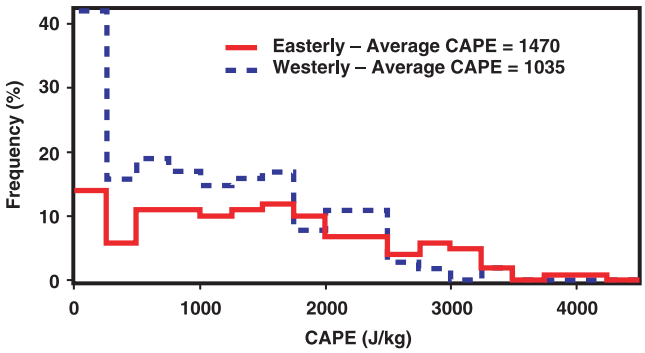


**Figure 9.** Distributions of CAPE values based on thermodynamic soundings at the ABRACOS site for the easterly and westerly wind regimes during the wet season January–February 1999.

by combining the ground stroke counts from the BLDN and the radar daily-integrated rainfall over the same area. The lightning yield is defined as the ratio of these two quantities and is given in convenient units of lightning strokes per $10^{12}$ kg of rainfall, as shown in Figure 8.

### 3.4. Thermodynamic Surface Measurements and Upper Air Soundings

[30] Surface meteorological measurements were collocated with the soundings at the ABRACOS pasture site 2 km SSW from the TOGA radar. During January and February 1999, sondes were released at 3-hour intervals, with some occasional interruptions in this schedule. Measurements of temperature and humidity at the 1-m level were used to characterize the surface parcels in the evaluation of convective available potential energy by the standard pseudoadiabatic process.

[31] Figure 9 shows the comparison in CAPE distributions for the easterly and westerly regimes. The distribution-integrated mean CAPE is greater in the easterly wind regime than the westerly regime, consistent with the flash rate behavior (Figure 6) and the behavior of stroke yield per unit rainfall (Figure 8), but the difference in the mean values is only 250 J/kg. Independent computations of CAPE with the same soundings by *Halverson et al.* [2002] show good agreement on the systematic differences between easterly and westerly regimes, though some effort was made in this other study to identify locally "disturbed" conditions and eliminate these soundings from the regime statistics. In the regime comparisons here, all soundings were used. A possible key feature of both sets of comparisons is the systematic difference in the tails of these distributions where in nearly every bin above 1000 J/kg the easterly wind regime is more strongly represented. The importance of the 1000 J/kg threshold is clarified by a comparison of CAPE and the previously discussed peak flash rates on individual days.

[32] Figure 10 shows the relationship between maximum CAPE and peak flash rate on individual wet season days. A CAPE threshold for lightning near 1000 J/kg is evident, with only one nonzero flash rate paired with a CAPE value smaller than this threshold. A distinction is also apparent here between green ocean (westerly) days in which the flash

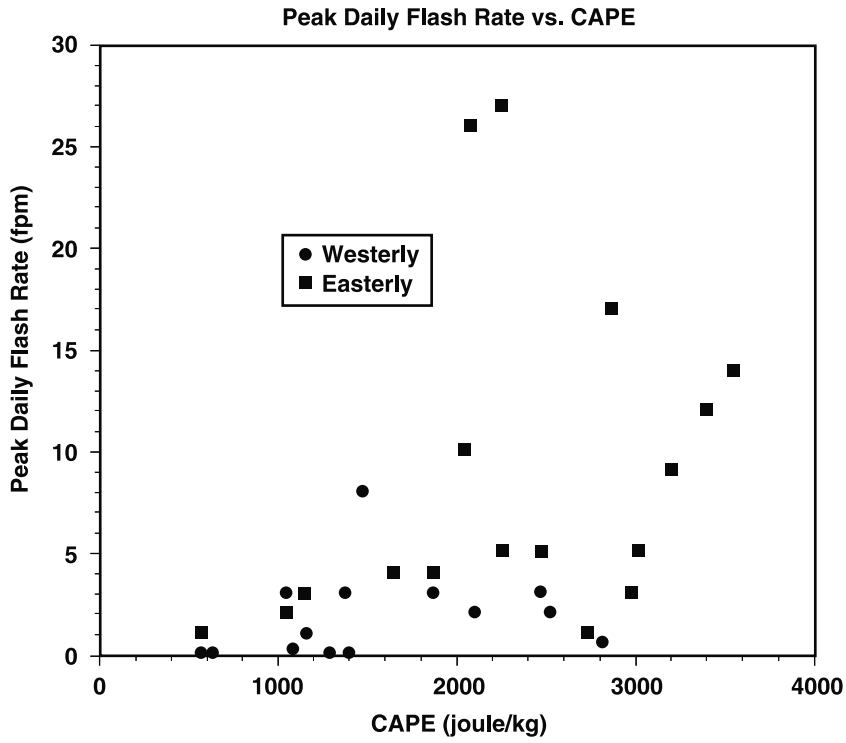


**Figure 10.** Maximum daily total flash rate versus maximum recorded convective available potential energy (CAPE) during the wet season (January–March 1999). Green ocean westerly days are distinguished from easterly regime days.

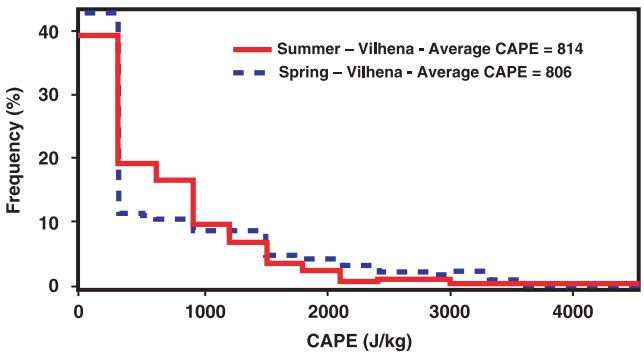


**Figure 11.** Distribution of CAPE values for Vilhena, Rondonia, for the wet season ("summer," January/February) and for the premonsoon season ("spring," October/November).

rates and CAPE tend to be small and the easterly days for which these values tend to be high. The days with flash rates greater than 10 fpm are all continental-style easterly days with CAPE greater than 2000 J/kg. Despite considerable scatter, the data show that CAPE and peak flash rate are positively correlated.

[33] During the premonsoon period (October–December 1999), no local thermodynamic soundings were available. A large collection of archived soundings from Vilhena (300 km distant; see the map in Figure 4) in earlier years (1967–1993) was therefore examined to compare the stability of the atmosphere during the premonsoon months (October and November of all years) and the wet season months (January and February of all years) for a lengthy interval (1967–1993). These soundings were performed at 1200 UTC (0800 local time), thereby discouraging direct comparisons of CAPE with the field program measurements on account of the substantial diurnal variation of CAPE at land stations. It was, however, possible to make absolute CAPE comparisons at a common local time between the wet season months and the premonsoon months, with thousands of soundings. The comparative CAPE distributions are shown in Figure 11. These comparisons show a similar behavior to the easterly/westerly comparison. The distributions of mean CAPE values are nearly the same, but in the tail of these distributions (i.e., above the inferred threshold value of 1000 J/kg) nearly every bin shows a larger number in the premonsoon period than during the regular wet season. These comparisons are qualitatively consistent with the peak flash rate comparisons in Figure 6 and with the extraordinarily deep thunderstorms observed with radar in both October and November.

### 3.5. Satellite Analysis of Cloud Microphysics

[34] Cloud microstructure and precipitation-forming processes, which are known to be influenced by updraft and by aerosol, were examined by using the methodology of *Rosenfeld and Lensky* [1998] and *Rosenfeld and Woodley* [2000]. AVHRR satellite observations over Brazil were gathered and studied for several days during the four meteorological regimes summarized in Table 1 and targeted in this study. A principal quantitative result is the temperature ($T$) dependence (or equivalently, the altitude dependence) of the cloud droplet effective radius ($r_{eff}$). These observations enable the classification of microphysical regimes (diffusional growth, coalescence, rainout, and glaciation), which are of central importance in testing hypotheses. The classification algorithm uses the thirtieth percentile of the $r_{eff}$ distribution at any given $T$. Application of the classification to lower percentiles shifts the classification to clouds with smaller $r_{eff}$, which are typically younger and with less ice. Therefore the $T$ range of microphysical zones for a given percentile depends on the maturity of the cloud population in the selected area. The numbers in Table 2 are selected from cloud areas with relatively young elements, to match our interest in the microstructure of the growing convective elements containing supercooled water and electrification processes.

[35] Table 2 summarizes the days for which data were extracted. Each day includes a summary of the AVHRR parameters previously discussed by *Rosenfeld and Lensky*

**Table 2.** Summary of AVHRR Satellite Case Studies Over Rondonia, Brazil, for 1999[a]

| Date in 1999 | Time, UT | Regime | Diffuse Growth | Active Coalescence | Rain-out | $r_{eff}$, 10°C μm | $r_{eff}$, −10°C μm | $T_g$, °C | $T_{top}$, °C | CCN, $cm^{-3}$ | CN, $cm^{-3}$ | Yield, $N/10^{12}$ kg |
|---|---|---|---|---|---|---|---|---|---|---|---|---|
| 6 Jan. | 1837 | W | No | Yes | Yes | 15 | 25–30 | −10 | −81 | 220 | | |
| 15 Jan. | 1937 | W | No | Yes | Yes | 20–23 | 25–30 | −8 | −89 | 380 | | |
| 19 Jan. | 1934 | W/E | No | Yes | No | 15–18 | >30 | −13 | −80 | 750 | | 1100 |
| 20 Jan. | 1922 | E | No | Yes | No | 14–19 | 25–30 | −20 | <−90 | 770 | | 23 |
| 12 Oct. | 1959 | PP | Yes | No | No | 5–7 | 15 | −35 | −89 | | 7700 | 4600 |
| 13 Oct. | 1947 | PP | Yes | No | No | 7–10 | 15–18 | −38 | −81 | 3600 | 5500 | 650 |
| 15 Oct. | 1924 | PP | Yes | No | No | 7–9 | 17–22 | −26 | −88 | 2700 | 4600 | 1300 |
| 19 Oct. | 2020 | PP | Yes | No | No | 7–10 | 15–20 | −26 | −89 | 2800 | 6000 | 14,100 |
| 20 Oct. | 2008 | PP | Yes | No | No | 7–12 | 10–15 | −32 | <−90 | 2600 | 12,400 | 8100 |
| 24 Oct. | 1922 | PP | No | Yes | No | 18 | 25–30 | −29 | −88 | 1500 | 2200 | 5000 |
| 29 Oct. | 2007 | CP | No | Yes | No | 8–9 | 25–30 | −28 | −77 | 500 | | 2200 |
| 2 Nov. | 1921 | CP | No | Yes | <−5C | 17–22 | 20–25 | −24 | −89 | | | 2900 |
| 15 Nov. | 2015 | CP | No | Yes | No | 9–12 | 25–30 | −26 | −86 | 560 | 600 | 12,600 |
| 16 Nov. | 2003 | CP | No | Yes | No | 12 | 30 | −16 | <−90 | 670 | 450 | 6600 |
| 17 Nov. | 1952 | CP | No | Yes | No | 11–13 | 25–30 | −17 | −88 | 470 | 800 | 16,800 |
| 26 Nov. | 1950 | CP | No | Yes | small | 12–13 | 20 | −24 | <−90 | 950 | | 6500 |
| 29 Nov. | 1915 | CP | No | Yes | Yes | 22–27 | >30 | −12 | −88 | | | 11,000 |

[a] W, westerly; E, easterly; PP, polluted premonsoon; CP, clean premonsoon; $r_{eff}$, effective particle radius; $T_g$, glaciation temperature; $T_{top}$, minimum cloud top temperature; CCN, cloud condensation nuclei at 1% supersaturation; yield, daily strokes per $10^{12}$ kg of rainfall.

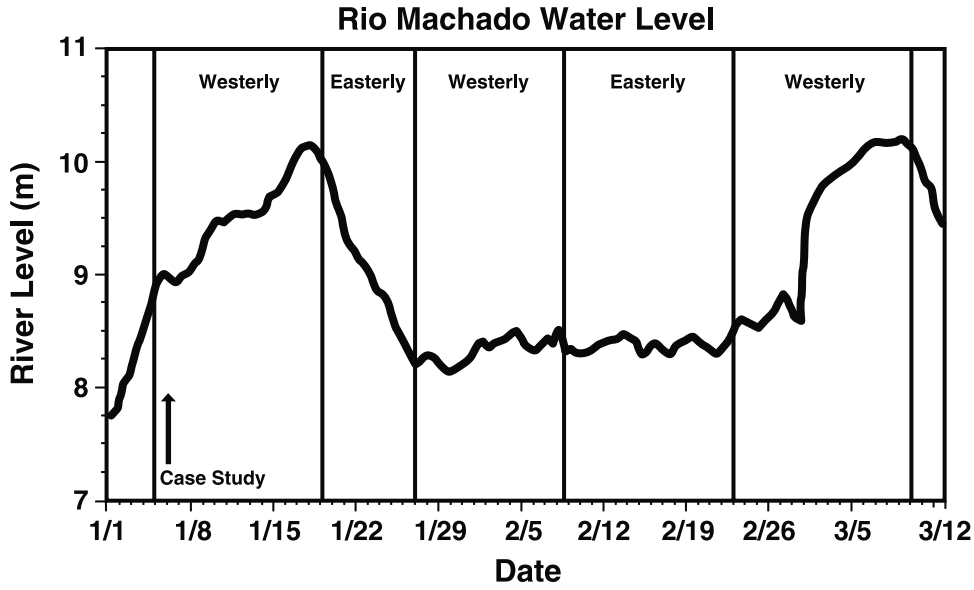


**Figure 12.** River stage in meters for the Rio Machado in Ji Parana, Rondonia. Also shown are the wet season regimes identified on the basis of wind analyses in of *Rickenbach et al.* [2002]. The day selected for a case study is indicated with an arrow.

[1998] and additional parameters that were used earlier to broadly characterize regimes. The observations will be used in the discussion of case studies in the following section.

## 4. Case Study Days

[36] From the long list of days examined with AVHRR data in Table 2, three specific days are presented as case studies to document three modes of physical behavior: (1) 6 January 1999, pronounced maritime behavior with very low CCN air, termed here the "green ocean" regime; (2) 17 November 1999, continental behavior in the premonsoon regime in which the CCN count is as low as the average value of the westerly regime, but for which the effects of the updraft appear to dominate the effects of the aerosol in the microphysical development and electrification; and (3) 12 October 1999, highly polluted continental behavior consistent with the predictions of the aerosol hypothesis showing evidence that aerosol suppresses coalescence in the warm phase and affects the mixed phase electrification in ways yet to be fully quantified.

[37] Figures 12 and 13 show the regime context for these three selected days, with the use of the continuous Rio Machado river stage observations that reflect changes in regional rainfall. Recorded at the BR 364 highway bridge in Ji Parana (see Figure 4), this river level responds to rainfall in a natural drainage overlapping with the TOGA radar surveillance.

[38] Figure 12 shows the entire wet season for 1999 with denotation of the periods of easterly and westerly wind regimes drawn from Table 1. The general relationship between river stage and regime is readily apparent, with the green ocean westerly regime characterized by a rising river level (with total changes in excess of 2 m), whereas during the easterly regime, the river level is either stable or declining. The first pronounced westerly episode occurred during 6–7 January for which 66 mm of rainfall was recorded at the TOGA radar site within a 24-hour period. The selected case study day of 6 January is marked in Figure 12.

[39] Figure 13 shows the same river stage record for the premonsoon interval, October–November 1999. Note that the October level is some 2 m less than the level within the wet season in Figure 12. Also shown is a simultaneous record of daily mean CCN concentration, which is more complete than that during the earlier wet season. October is heavily polluted as a result of post–dry season biomass burning with values exceeding 5000 CCN $cm^{-3}$ in early October, when the disc of the Sun often could not be discerned. The boundary layer in November is, however, remarkably clean, with some daily mean values less than 500 CCN $cm^{-3}$ and hence almost as clean as the westerly wind regime in the earlier wet season. These measured pollution levels were mirrored by the clarity of

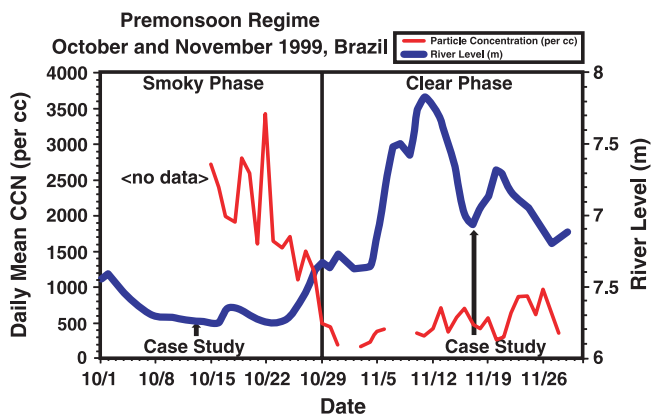


**Figure 13.** Simultaneous records of the Rio Machado river stage and mean daily CCN concentration for the transition months of October and November 1999. Days selected for case studies are indicated with arrows.

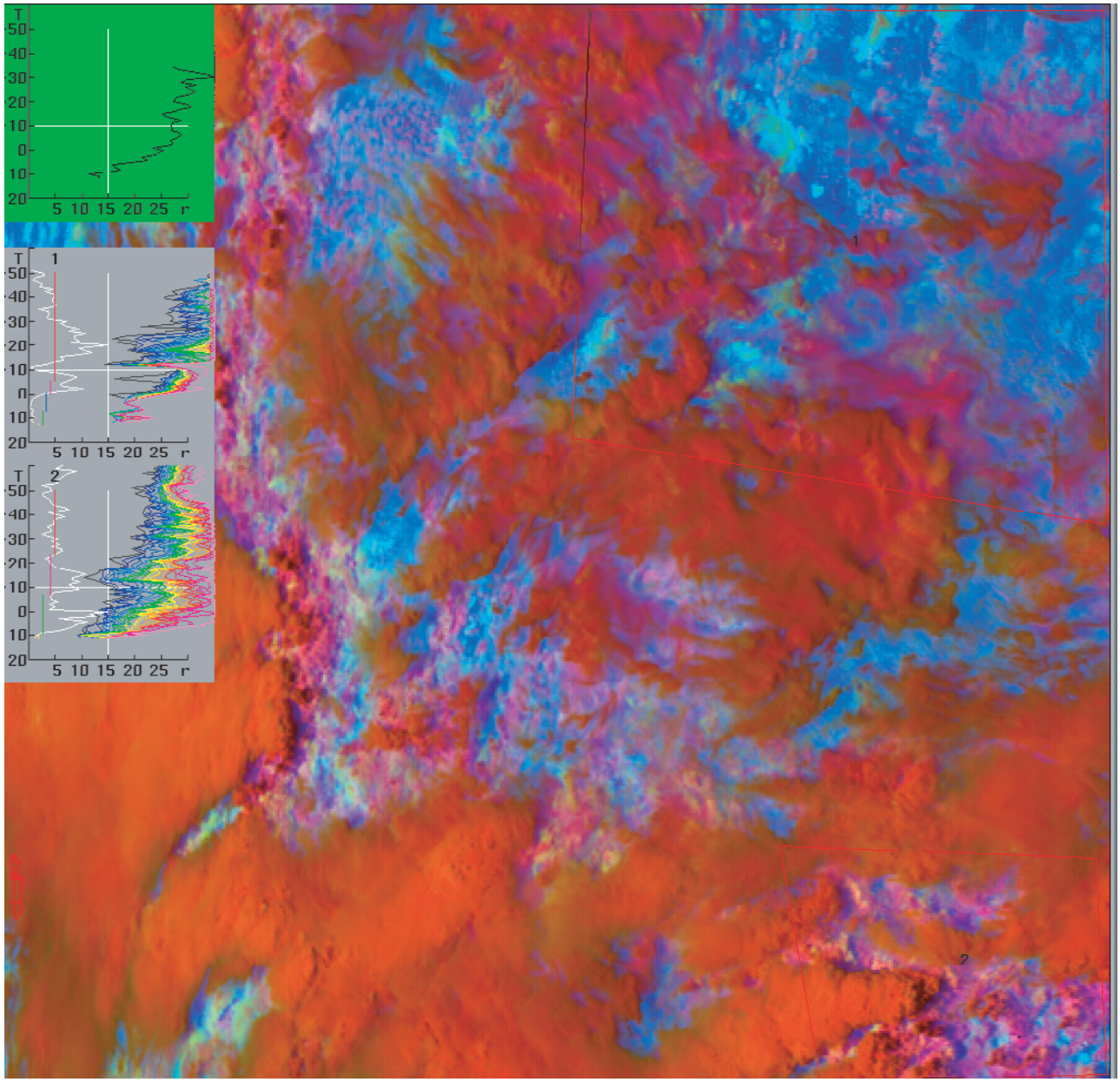


**Figure 14.** AVHRR image for 6 January 1999, 1837 UT, during the green ocean regime. The image covers about 500 × 500 km centered over the LBA area. The color scheme shows qualitatively the microphysical structure, using the methodology of *Rosenfeld and Lensky* [1998]. The color scheme is red for the visible, green for the 3.7-μm reflectance component, and blue for temperature. The ship tracks with reduced particle size appear as cloud bands of enhanced green, or enhanced 3.7-μm reflectance. The $T$-$r_{\text{eff}}$ relations and the microphysical zones are provided in the inset graphs. The microphysical zones are denoted by the vertical bars at the left of the graphs: 1, diffusional growth; 2, coalescence; 3, rainout; 4, mixed phase; and 5, glaciated cloud.

the atmosphere and the ability to see clearly a small hilltop in Ouro Preto from Abracos Hill at a distance of 10 km. This hilltop was often totally obscured by smoke aerosol during October. One selected case study day is marked for 13 October in the highly polluted period in the first half of October, just as our measurements were getting under way and the river level was at minimum. The onset of rainfall in the transition season in late October was responsible for the cleansing of the atmosphere from October into November, as this record demonstrates. The river stage is clearly rising as the pollution level declines. This evolution is probably accelerated by two effects: the rainfall suppression of fire throughout Rondonia and nearby Mato Grosso (either directly or by the moistening of the vegetation), which is the main source of boundary layer aerosol, and the condensation/precipitation process in natural moist convection,

which efficiently removes cloud condensation nuclei from the atmosphere. The case study selected in this clean premonsoon phase is 17 November.

### 4.1. 6 January

[40] This day is a well-defined green ocean, with abundant rainfall (76 mm at the radar site in a 24-hour period), a rising river level (Figure 13), very little lightning activity (only three flashes were detected all day), and CCN concentrations at times as low as the blue ocean (<100 $cm^{-3}$). The daily mean CCN concentration was 220 $cm^{-3}$.

[41] The AVHRR image of 6 January (Figure 14) reveals relatively featureless cloud tops, suggesting that they lacked convective vigor, which in turn suggests the existence of only modest updrafts. The minimum cloud top temperature of −81°C, while still a very low value in absolute terms, was the warmest of all the cases examined. The steep increase of the effective radius of cloud particles low in the cloud indicates the existence of active coalescence starting above cloud base, in agreement with the low CCN concentrations. Strong coalescence was associated with an indicated rainout zone, suggesting that resultant warm rain was falling through the updrafts. The indicated glaciation temperature of more than −10°C was consistent with the depleted supercooled water, due to the weak updrafts with strong coalescence, leading to rainout.

[42] The AVHRR observations are consistent with the precipitation structure disclosed with radar RHI scans (Figure 15). The reflectivity is a moderately large 40 db*Z* at low levels, consistent with active coalescence, but in the mixed phase region (in this case, above 4.5-km altitude) it is commonly only 20 db*Z*, with occasional 30 db*Z* over small (a few kilometers scale) volumes. This structure is characteristic of maritime conditions [*DeMott and Rutledge*, 1998] and is similar to observations in the monsoon regime in Australia [*Williams et al.*, 1992; *Rutledge et al.*, 1992]. This storm exhibited no lightning.

### 4.2. 17 November

[43] Following a period of active premonsoon rainfall (Figure 13), the boundary layer air for this case is characterized by a mean CCN concentration of 470 $cm^{-3}$, twice as large as the value on 6 January but on a par with the median values in the westerly regime (Figure 5). The mean CN concentration is 800 $cm^{-3}$, similar to values over much of the blue ocean (Figure 1).

[44] The cloud top visible imagery in Figure 16 shows a much more "boiling" appearance and colder minimum temperature (−88°C) compared with 6 January, indicating greater vigor and stronger updrafts. The smaller effective radius of the droplets at the warm part of the cloud was well above the 15-μm threshold of coalescence but without any indication for a rainout zone. The smaller low-level droplets and the lack of rainout zone can be attributed to both a larger concentration of CCN and stronger updrafts. With no rainout, all cloud condensate is raised to the supercooled levels. The large supercooled drops fully glaciated at about −17 to −22°C. This means a mixed phase zone twice the depth of the 6 January case.

[45] These AVHRR observations are again consistent with the cloud structure observed by radar. The RHI scan in Figure 17 shows pronounced continental structure, with a maximum cloud top exceeding 19 km. Strong mixed phase development is evident with 30-db*Z* reflectivity extending to 15-km altitude. This storm's distance from the radar prevented an estimate of peak flash rate. Other giant thunderstorms with radar tops exceeding 16 km were noted on 26 occasions in clean November and on five occasions exceeded 19 km, and these storms are responsible for the strong tails in the peak flash rate histograms for the premonsoon in Figure 6. Cloud top heights of this magnitude were seldom reported in the earlier wet season.

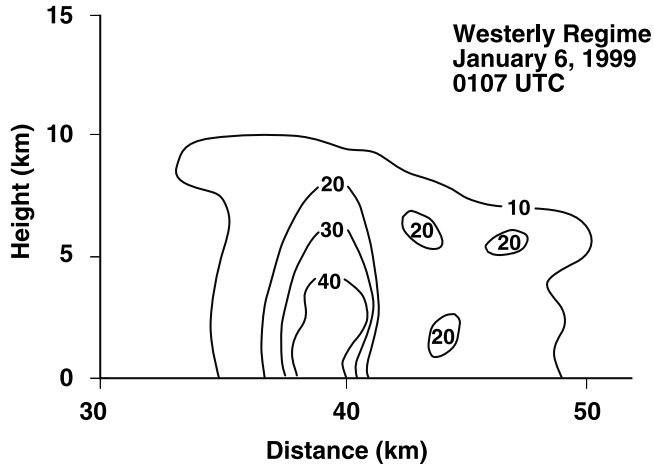


**Figure 15.** TOGA radar RHI scan on 6 January 1999 in the green ocean regime showing vertical development characteristic of maritime convection. No lightning was observed at this time.

### 4.3. 13 October

[46] Large scattered thunderstorms progressed from east to west, ingesting highly polluted air with smoke, with daily mean CCN and CN concentrations of 3600 and 5500, respectively, among the highest values recorded in the field program. The appearance of the cloud tops in the cloud imagery for this case (Figure 18) is intermediate between the boiling appearance on 17 November and the featureless appearance on 6 January, suggesting an intermediate extent of the vigor and updrafts. The minimum cloud top temperature reached −89°C, similar to the value on 17 November. The extremely small values of the effective radius, well below 10 μm and the smallest values in Table 2, extended through the 0°C isotherm, showed the profound impact of the extremely high concentration of CCN on creating very small cloud droplets and practically shutting off the coalescence in the warm part of the cloud. The indicated effective radius remained mostly below 15 μm up to the −10°C isotherm, implying that the lower boundary of the mixed phase zone started at that elevated level relative to the other cases. The glaciation temperature was shifted correspondingly to lower temperatures, ranging from −22°C to −38°C, at different areas of thunderstorms. It is noteworthy that the glaciation temperature of −38°C coincides with the temperature of homogeneous freezing and hence the lowest possible value on theoretical grounds. The existence of such values was confirmed elsewhere by aircraft observations [*Rosenfeld and Woodley*, 2000]. In this

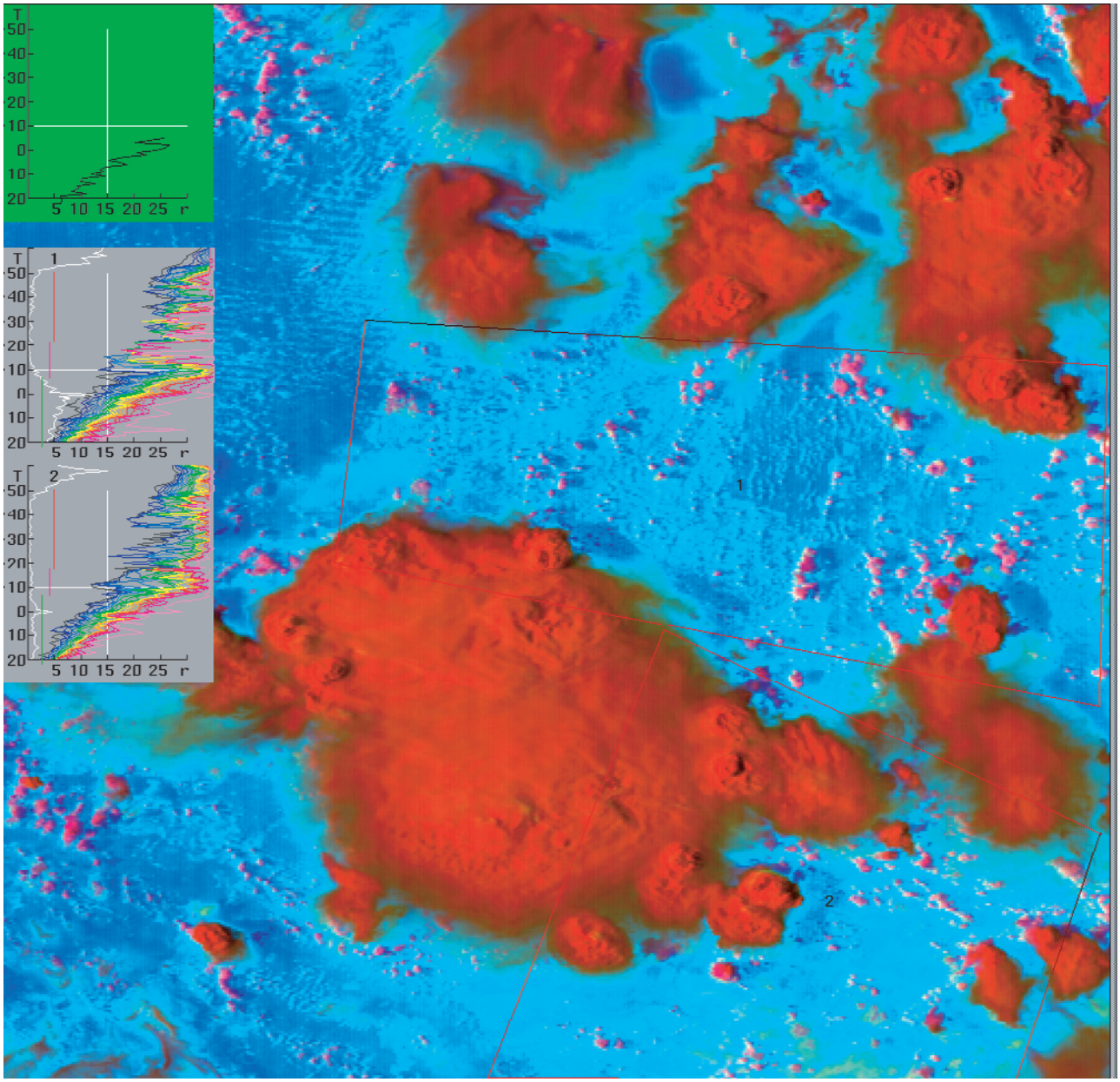


**Figure 16.** Same as Figure 13, but for the AVHRR overpass on 17 November 1999, 1952 UT, during the premonsoon easterly regime in relatively clean atmosphere.

case, there is little doubt that all condensates were lofted to the supercooled levels without any loss to precipitation. However, ice was evidently more scarce in comparison with the other cases in the 0 to −20°C levels, and this may have implications for the electrical activity.

[47] Some peculiar aspects of the lightning activity were noted from the radar site. Some of these observations are of a very qualitative nature but are still worthy of documentation, given the rather extreme aerosol conditions. As the squall line approached from the east, numerous small field changes were detected, with a peak rate of 27 fpm, but no thunder was noted. Nor was any lightning seen visually. Examination of the BLDN data for this day (not shown) showed very sparse ground flashes (only 45 flashes within 150-km range of the radar in the same hour of the total lightning observations). Approximately half of these ground flash identifications showed positive polarity, the exceptional polarity for ground flashes in general. Closer examination of the peak currents for these positive events showed values of generally less than 6 kA. This evidence suggests that these flashes were in reality intracloud flashes masquerading as positive ground flashes. The following evening, 14 October, isolated thunderstorms were observed directly overhead in Ji Parana from the rooftop of the Hotel Transcontinental. A maximum flash rate of 8–10 fpm was observed, but no ground flashes were seen. (Consistent with this observation, the BLDN recorded not a single ground flash within 20 km of Ji Parana during the time of these observations.) All of the lightning appeared to be intracloud flashes of short duration, and little if any thunder was heard, consistent with the daytime observations

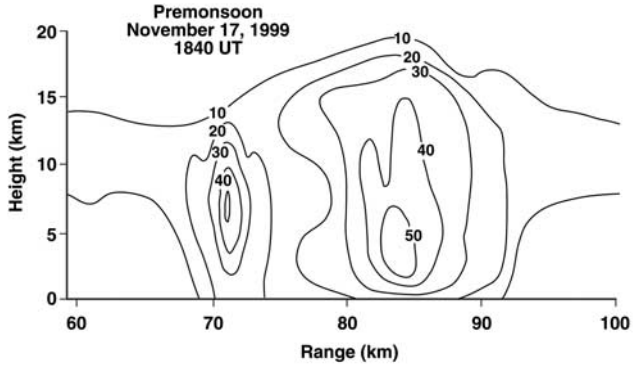


**Figure 17.** TOGA radar RHI scan through a giant thunderstorm on 17 November 1999.

on the previous day. Only light rain was detected from these storms. It is possible that these observations are symptomatic of a mixed phase microphysics appreciably modified by the effect of the smoke.

## 5. Relationship Between Lightning Yield and Aerosol During the Wet Season

[48] Earlier regime comparisons in Australia [*Williams et al.*, 1992; *Rutledge et al.*, 1992] often showed large differences in daily rainfall between the monsoon ("maritime") regime and the break period ("continental") regime. *Cifelli et al.* [2002], *Halverson et al.* [2002], and *Petersen et al.* [2002] found more modest rainfall differences between easterly and westerly regimes in Brazil, but the most extreme westerly

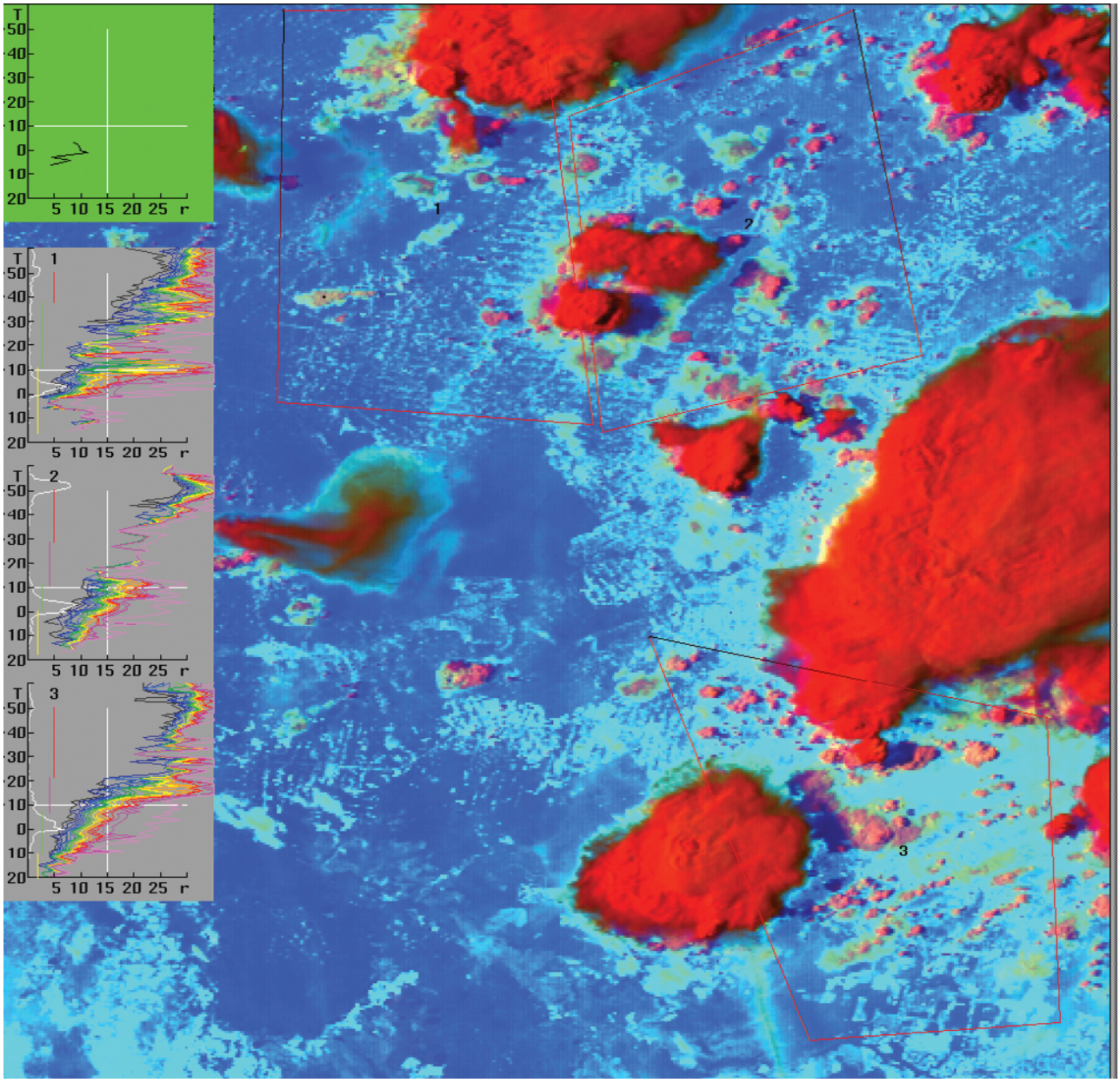


**Figure 18.** Same as Figure 13, but for 13 October 1999, 1947 UT, with a strongly polluted boundary layer. Evidence for diffusional growth of cloud droplets is apparent, and a deep layer indicates the suppressed coalescence.

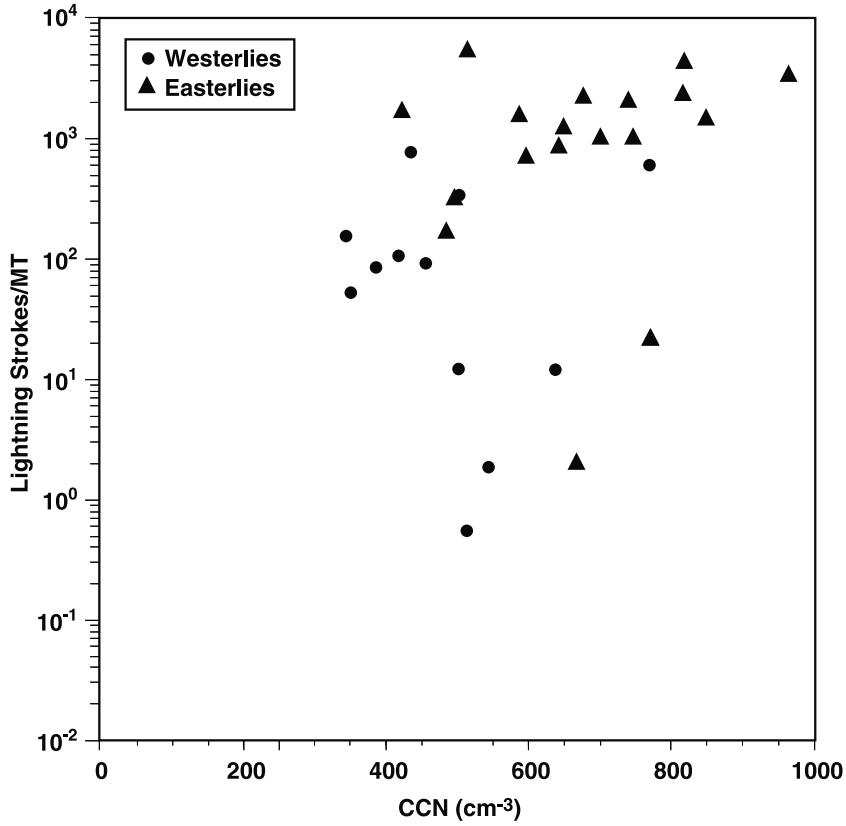


**Figure 19.** Comparison of lightning stroke yield per unit rainfall (within 100-km radius of the TOGA radar) and mean CCN concentration for individual days within the 1999 wet season. Easterly and westerly days are distinguished by symbols.

event in 1999 on 6 January, chosen with the clearest indication of green ocean behavior, produced the greatest daily rainfall total during the 1999 wet season. A key distinction of the green ocean response is the widespread nature of the rainfall.

[49] Tests of the aerosol hypothesis for electrification between regimes and within a regime benefit from a normalization of the rainfall: the daily lightning stroke yield per unit rainfall. A comparison of yield versus daily CCN concentration (both measurements centered on the TOGA radar location) for all available days in the 1999 wet season is shown in Figure 19. Despite considerable scatter, clear evidence for positive correlation is evident, both regime to regime, and within the more highly electrified easterly regime. The apparent sensitivity is substantial over a range of CCN concentration that bridges the range between general maritime and continental conditions (100–1000 $cm^{-3}$) and amounts to more than a tenfold change for a doubling of CCN concentration.

[50] The interpretation of these results is unfortunately ambiguous and will be addressed in the following discussion section.

## 6. Discussion

[51] Four distinct meteorological regimes in Brazil have been examined with multiple observations to distinguish a role for aerosol and instability (CAPE). The regime-to-regime trends in CAPE follow like trends in all measures of cloud electrification: lightning peak flash rate, cloud-to-ground stroke count (see also *Petersen et al.* [2002]), and lighting yield per unit rainfall. The westerly green ocean regime is most maritime, the easterly regime is intermediate, and the premonsoon regime is most continental. The predominance of lightning activity in the premonsoon period is consistent with earlier thunderday reports over the Amazon region [*World Meteorological Organization*, 1956]. The regime-to-regime trends in CCN concentration also follow this ordering, but with one crucial exception: the lightning-active November premonsoon phase with a relatively clean boundary layer. This CCN-poor and lightning-active regime casts doubt on a leading role for the aerosol in explaining a decidedly continental behavior in both lightning and radar structure. In the presence of large CAPE and attendant updraft, it is expected that the aerosol cannot play a primary role.

[52] Giant, lightning-active thunderstorms were documented in the November period. Climatologically speaking, the CAPE values in this period (Figure 10) are among the highest in Rondonia and are clearly greater than values in the green ocean westerly regime (Figure 8). These observations together support a fundamental role for the updraft and suggest that aerosol is not always essential for continental cloud structure and active lightning. In view of the evidence so far, the direct factor determining the extent of cloud electrification is the cloud water that rises to the supercooled zone with the updraft. The lack of rainout of the cloud water from the updrafts during the low-CCN

premonsoon shows that the updrafts are sufficiently strong to bring the water to the supercooled zone before much water is lost by rainout process. That renders superfluous the alternative process of preventing rainout by aerosols suppressing the coalescence and warm rain.

[53] Evidence consistent with specific predictions of the aerosol hypothesis was documented in the most polluted (early) phase of the premonsoon, namely, the complete suppression of warm rain coalescence. Furthermore, satellite evidence was found that the mixed phase was subsequently activated by the arrival of cloud liquid water content from lower levels, leading to moderately active intracloud activity, but with relatively weak discharges. Evidence for weaker than average electrification overall (consistent with aerosol concentrations beyond an optimal level for electrification) was found in the lightning yield per unit rainfall, which was substantially smaller than the mean value for the premonsoon regime (5700 strokes per $10^{12}$ kg of rainfall). It seems probable that the same small cloud droplets that led to the suppression of coalescence also suppressed (1) the growth of graupel particles in and/or (2) the delivery of large supercooled raindrops to the mixed phase region and thereby deterred vigorous charge separation.

[54] Thunderstorms growing from highly polluted boundary layer air in early October showed evidence for suppressed coalescence throughout the "warm" region of the cloud. Consistent with the predictions of the aerosol hypothesis in Figure 1, these observations demonstrate the delivery of colloidally stable cloud water to the mixed phase region where it is then available for precipitation growth by ice microphysics. Furthermore, the glaciation is delayed because the smaller cloud droplets freeze at colder temperatures and are also collected less efficiently by ice hydrometeors. The concentrated CCN appear to be essential to explaining these observations, and the updraft then plays a secondary role. The aerosol's role in enhancing cloud electrification is placed in doubt by the stroke yield per unit rainfall, which was substantially smaller for these 2 days than the mean for all the premonsoon days. This observation may indicate that the aerosol concentration is beyond optimal levels, as suggested in section 1.3. The observed peak flash rate on 13 October was much higher than green ocean peak rates (Figure 6), though not as high as values observed in the less polluted November premonsoon. The lightning also appeared to be unenergetic, with few ground flashes. The aerosol-rich small droplet mechanism that assures colloidal stability in the warm part of the cloud and thereby assures the delivery of cloud water by updraft to the mixed phase region may work against the active riming process needed for creating large concentrations of graupel and ice crystals, which are required for vigorous charge separation and active energetic lightning, at least at temperatures $>-20°C$. Further studies of this highly polluted regime are needed to support these speculations. It is also important to emphasize the extreme nature of the pollution in this regime. Fires were still prevalent throughout Rondonia and the CN counter readings were generally in the range 5000–10,000 $cm^{-3}$, with frequent saturation of the instrument at 30,000 $cm^{-3}$. The comparison of these readings with the CN climatology in Figure 1 strongly supports the "supercontinental" label for this early October regime.

[55] The physical interpretation of observations during the wet season remains ambiguous but is well worth addressing because integrated observations of this nature for a tropical continental zone have not been previously examined. The trends in CCN concentration (Figure 5), CAPE (Figure 9), and lightning (Figures 6–8) are all the same. The regime with the cleanest air, the least CAPE, and the least lightning activity is the green ocean westerly regime. Lightning yield per unit rainfall is positively correlated with CCN concentration throughout the wet season, but cause and effect cannot be resolved with the observations now available. The results in Figure 19 could be interpreted in favor of the aerosol hypothesis, or alternatively, as an effect of the convection and rainfall on the boundary layer. The green ocean convection is areally extensive and effective at mixing the troposphere and thereby diluting the CCN concentration (see also *Roberts et al.* [2001]). Extensive convection and rainfall will be efficient in removing the aerosol from the atmosphere, a likely contributor to the declining CCN concentration from October to November documented in Figure 13. The troposphere of the more unstable easterly regime is less well mixed and could therefore sustain a more polluted boundary layer and, at the same time, an enhanced moist entropy with larger CAPE.

[56] Because of the remaining ambiguity surrounding the Amazon wet season, the green ocean deserves further discussion. The existence of a predominantly maritime regime over a large continent is unexpected to students of atmospheric electricity who have long recognized South America as one of the three major tropical sources (with Africa and the Maritime Continent) for the global electrical circuit [*Whipple*, 1929] and arguably the predominant source for the DC global circuit. On this basis, continental style convection is expected with active lightning. In fact, the resemblance of the lightning sparse and rainfall abundant green ocean to actual oceanic convection is obscured in seasonal climatologies [e.g., *World Meterological Organization*, 1956] since individual months are invariably influenced by the lightning-active easterly regime that alternates frequently with the green ocean (westerly) regime (Figure 12).

[57] Given the weight of evidence in the paper for the traditional CAPE-based hypothesis for the land-ocean lightning contrast, it is appropriate to examine other evidence against this idea. For example, it has been suggested that CAPE over warm ocean water is the same as that over land [*Lucas et al.*, 1996; *Zipser*, 2002], and still the maritime lightning is much reduced, if not absent. Further evidence for a similarity in CAPE at land and ocean stations was documented even earlier [*Williams and Renno*, 1993]. However, none of these studies has considered the subtleties of the diurnal variation of boundary layer moist entropy over land and over ocean. The order-of-magnitude diurnal variation in lightning over land is well recognized [*Williams and Heckman*, 1993], in marked contrast to the often indiscernible variation over oceans. The diurnal variation in wet bulb potential temperature during the easterly regime in Brazil was of the order of $1°–2°C$, equivalent to 1000–2000 J/kg of CAPE [*Williams and Renno*, 1993]. These values are already larger than the mean CAPE contrast between Amazon's easterly and westerly regimes (500 J/kg) and between the wet season and the premonsoon.

[58] Possible further evidence against the CAPE-based hypothesis is the observation that a strong climatological

land-ocean lightning contrast persists at nighttime [*Orville and Henderson*, 1986], when the contrast in CAPE is less viable than a contrast in boundary layer aerosol concentration. However, nighttime lightning over land is often occurring when deep convection was suppressed for some reason during the day, allowing for substantial residual instability as a driver for the nighttime lightning.

[59] The observation of substantial contrasts in peak flash rate (Figure 6) and lightning yield per unit rainfall (Figure 8) between regimes, in contrast with only subtle changes in CAPE (*Halverson et al.* [2002] and this study), is further evidence that lightning activity is sensitive to small changes in cloud buoyancy.

## 7. Conclusions

[60] The comparison of lightning activity in four distinct meteorological regimes in the Amazon region has enabled new tests of the aerosol hypothesis for cloud electrification. The documentation of comparable electrical parameters during two distinct months of the most electrically active premonsoon regime (one month (October) dominated by boundary layer smoke and one month (November) showing low CCN concentration) casts doubt on a primary role for the aerosol in enhancing the electrification. The climatological evidence for maximum CAPE during the premonsoon phase supports the traditional hypothesis for lightning control.

[61] The observations also demonstrate strongly suppressed coalescence and prevention of rainout in highly polluted conditions in the early premonsoon. Superhigh concentrations of CCN were already documented elsewhere to suppress coalescence and ice precipitation [*Rosenfeld*, 2000; *Rosenfeld and Woodley*, 2002; *Khain et al.*, 2001]. There are indications that such clouds actually lack sufficient ice for cloud charging processes at $T > -20°C$, delaying the electrically active vertical zone of the cloud to higher altitudes. The character of the observed lightning discharges in these clouds is consistent with this suggestion.

[62] The more moderate CCN concentrations of the easterly regime, in a range between the green ocean values and these highly polluted levels, may similarly prevent rainout by slowing coalescence. The lightning yield per unit rainfall is positively correlated with CCN concentration in this regime. However, CAPE and CCN are expected to be correlated for reasons attributable to tropospheric overturn, and the observations available here (not shown) support this expectation. For lack of sufficient quantitative observations, the relative contributions of the hypothesized aerosol effect and the updraft could not be determined.

[63] The green ocean westerly regime contrasts most strongly with the premonsoon regime and more closely resembles the real oceanic convective regime than any other regime over land. This is telling us something. The very possibility of an ocean-like tropical convective regime well inland, over inhomogeneous terrain that is not even completely flat, suggests that the fundamental cause for the oceanic regime is not entirely attributable to differences in surface properties between land and ocean and that other factors are playing a role. Therefore it is likely that major factors that are fundamental to the causes of the consistent maritime nature of convection over the blue ocean, characterized by weak updrafts and little if any lightning, are yet to be discovered.

[64] **Acknowledgments.** Numerous individuals contributed to the success of the field program in Brazil. Generous logistical support from Joao Luiz Esteves (008) and Eduardo Conceicao de Locerda (007) of INCRA was invaluable. E. Amitai, R. Bowie, C. Christina, R. Ferreira, Z. Haddad, P. Kuchera, C Morales, E. Plows, L. Pereira, R. Toracinta, and J. Wang all devoted many hours to radar operations. Gilberto Fisch enthusiastically encouraged student participation. Coordination with the crew at the ABRACOS site, including M. Garstang, B. Ferrier, D. Penny, R. Heitz, J. Tota, and J. Sigler, enhanced the value of simultaneous data sets. Jim Wilson provided able assistance in selection of radar sites, Jon Lutz loaned radar equipment, Bob Boldi organized data acquisition systems, Elizangela de Araujo Silva filled gaps in the river record, Marx Brook and Dave Rust loaned field change antennae, John Hall and Karen Rothkin produced figures, and Jose Rosa provided assistance with the meteorological data archive in Brasilia. R. Barchet and N. Laulainin of Battelle Laboratories generously loaned the CCN counter for this field program. E. Betterton, S. Twomey, and G. Shaw provided valuable instruction and advice in its operation and maintenance. J. Beck, T. Germano, A. L. Loureiro, E. Fernandes, and A. Ribeiro devoted considerable time toward sustaining the operation of both particle counters. The Brazil Lightning Detection Network was established through the able assistance of Evandro Ferraz, Osmar Pinto, and the hard work of dozens of unnamed contributors in the Rondonian towns of Guajara-Mirim, Machadinho do Oeste, Vilhena, and Ouro Preto. Additional financial support for the BLDN was provided by Augusto Cesar Vaz de Athayde at INMET in Brasilia. We also thank Alaor Dell'Antonia for assistance with the meteorological data there. Valuable discussions on problems of aerosol and tropical convection with M. Andreae, M. Silva Dias, M. Baker, E. Betterton, L. Carey, A. Detwiler, J. Dye, P. Dias, B. Ferrier, M. Garstang, J. Hallett, L. Harrison, G. Heymsfeld, A. Hogan, J. Hudson, A. Khain, G. Lala, W. Lyons, D. MacGorman, R. Markson, R. Orville, S. Rutledge, R. Sagalyn, V. Schroeder, J. Stith, S. Twomey, G. Vali, J. Willett, and E. Zipser are appreciated. Steve Rutledge led the way across the Amazon from the U.S. side to make this program happen. Ramesh Kakar and Otto Thiele of NASA GSFC paid for it, on NASA grant NAG5-4778. P. Artaxo acknowledges support from FAPESP. M. de Agostinho acknowledges support from NASA Ames and from FAPESP. G. Roberts was supported by the Max Planck Institute of Chemistry. D. Rosenfeld and E. Williams acknowledge support from the U.S.-Israel Binational Science Foundation, grant 037-8274. Last, but far from least, the first author extends his appreciation to the families Carvalho de Souza, Dutra, and Vitorino (Ouro Preto); Esteves (Ji Parana); Avelino (Porto Velho); and Rosa, Coelho, and Oliveira (Brasilia) for their kind hospitality during the adventure in Brazil.

## References

Betts, A. K., J. Fuentes, M. Garstang, and J. H. Ball, Surface diurnal cycle and boundary layer structure over Rondônia during the rainy season, *J. Geophys. Res.*, *107*, 10.1029/2000JD000356, in press, 2002.

Black, R. A., and J. Hallett, Observations of the distribution of ice in hurricanes, *J. Atmos. Sci.*, *43*, 802–822, 1986.

Busness, K. M., A. A. Al-Sunaid, P. H. Daum, J. M. Hales, R. V. Hannigan, M. Mazurek, J. M. Thorp, S. D. Tomich, and M. J. Warren, Pacific Northwest Laboratory Gulfstream I measurements of the Kuwait oil-fire plume: July–August 1991, report, contract DE-AC06–76RLO 1830, Pac. Northwest Lab., Richland, Wash., Nov. 1992.

Christian, H. J., et al., Global Frequency and distribution of lightning as observed by the Optical Transient Detector (OTD), in *11th International Conference on Atmospheric Electricity*, *NASA/CP-1999-209261*, pp. 726–729, Guntersville, Ala., June 1999.

Churchill, D. D., and R. A. Houze Jr., Mesoscale updraft magnitude and cloud ice content deduced from the ice budget of the stratiform region of a tropical cloud cluster, *J. Atmos. Sci.*, *41*, 1717–1725, 1984.

Cifelli, R., W. A. Petersen, L. D. Carey, S. A. Rutledge, and M. A. F. Silva Dias, Radar observations of the kinematic, microphysical, and precipitation characteristics of two MCSs in TRMM LBA, *J. Geophys. Res.*, *107*, 10.1029/2000JD000264, in press, 2002.

DeMott, C. A., and S. A. Rutledge, The vertical structure of TOGA COARE convection, part I, Radar echo distributions, *J. Atmos. Sci.*, *55*, 2748–2762, 1998.

Fullekrug, M., and A. Fraser-Smith, Global lightning and climate variability inferred from ELF field variations, *Geophys. Res. Lett.*, *24*, 2411–2414, 1997.

Halverson, J., T. Rickenbach, B. Roy, H. Pierce, and E. Williams, Environmental characteristics of convective systems during TRMM-LBA, *Mon. Weather. Rev.*, *130*, 1493–1509, 2002.

Hogan, A., Meteorological variation of maritime aerosols, in *Atmospheric Aerosols and Nuclei*, edited by A. F. Roddy and P. C. O'Connor, pp. 503–507, Galway Univ. Press, Galway, Ireland, 1977.

Hudson, J. G., and S. S. Yum, Maritime/continental drizzle in small cumuli, *J. Atmos. Sci.*, *58*, 915–926, 2001.

Jorgensen, D. P., and M. A. LeMone, Vertical velocity characteristics of oceanic convection, *J. Atmos. Sci.*, *46*, 621–640, 1989.

Khain, A. P., D. Rosenfeld, and A. Pokrovsky, Simulating convective clouds with sustained supercooled liquid water down to −37.5°C using a spectral microphysics model, *Geophys. Res. Lett.*, *28*, 3887–3890, 2001.

LeMone, M. A., and E. J. Zipser, Cumulonimbus vertical velocity events in GATE, part I, Diameter, intensity and mass flux, *J. Atmos. Sci.*, *37*, 2444–2457, 1980.

Lucas, C., E. Zipser, and M. A. LeMone, Vertical velocity in oceanic convection off tropical Australia, *J. Atmos. Sci.*, *51*, 3183–3193, 1994.

Lucas, C., E. Zipser, and M. A. LeMone, Reply to "Comments on 'Convective available potential energy in the environment of oceanic and continental clouds'," *J. Atmos. Sci.*, *53*, 1212–1214, 1996.

Machado, L. A. T., H. Laurent, and A. A. Lima, Diurnal march of the convection observed during the TRMM-WETAMC/LBA, *J. Geophys. Res.*, *107*(X), 10.1029/2001JD000338, in press, 2002.

Markson, R. J., and D. Lane-smith, Global change monitoring through the temporal variation of the ionospheric potential, *AMS Conference on the Global Electric Circuit*, pp. 273–278, Am. Meteorol. Soc., Boston, Mass., 1994.

Orville, R. E., and R. W. Henderson, Global distribution of midnight lightning: December 1977 to August 1978, *Mon. Weather. Rev.*, *114*, 2640–2653, 1986.

Petersen, W. A., S. A. Rutledge, and R. E. Orville, Cloud-to-ground lightning observations from TOGA COARE: Selected results and lightning location algorithms, *Mon. Weather. Rev.*, *124*, 602–620, 1996.

Petersen, W. A., S. W. Nesbitt, R. J. Blakeslee, R. Cifeli, P. Hein, and S. A. Rutledge, TRMM Observations of intraseasonal variability in convective regimes over the Amazon, *J. Clim.*, *15*, 1278–1294, 2002.

Phillipin, S., and E. A. Betterton, Cloud condensation nuclei measurements in southern Arizona: Instrumentation and early observations, *Atmos. Res.*, *43*, 263–275, 1997.

Price, C., Global surface temperatures and the atmospheric electric circuit, *Geophys Res. Lett.*, *20*, 1363–1366, 1993.

Reeve, N., and R. Toumi, Lightning activity as an indicator of climate change, *Q. J. R. Meteorol. Soc.*, *125*, 893–903, 1999.

Reynolds, S. E., M. Brook, and M. Gourley, Thunderstorm charge separation, *J. Meteorol.*, *14*, 426–436., 1957.

Rickenbach, T. M., R. N. Ferreira, J. Halverson, D. L. Herdies, and M. A. F. Silva Dias, Modulation of convection in the southwestern Amazon basin by extratropical stationary fonts, *J. Geophys. Res.*, *107*(X), 10.1029/2001JD000263, in press, 2002.

Roberts, G., M. Andreae, J. Zhou, and P. Artaxo, Cloud condensation nuclei in the Amazon basin: "Marine" conditions over a continent?, *Geophys. Res. Lett.*, *28*, 2807–2810, 2001.

Rosenfeld, D., TRMM observed first direct evidence of smoke from forest fires inhibiting rainfall, *Geophys. Res. Lett.*, *26*, 3105–3108, 1999.

Rosenfeld, D., Suppression of rain and snow by urban and industrial air pollution, *Science*, *287*, 1793–1796, 2000.

Rosenfeld, D., and G. Gutman, Retrieving microphysical properties near the tops of potential rain clouds by multispectral analysis of AVHRR data, *Atmos. Res.*, *34*, 259–283, 1994.

Rosenfeld, D., and M. I. Lensky, Space-borne based insights into precipitation formation processes in continental and maritime convective clouds, *Bull. Am. Meteorol. Soc.*, *79*, 2457–2476, 1998.

Rosenfeld, D., and W. L. Woodley, Convective clouds with sustained highly supercooled liquid water down to −37.5°C, *Nature*, *405*, 440–442, 2000.

Rosenfeld, D., and W. L. Woodley, Closing the 50-year circle: From cloud seeding to space and back to climate change through precipitation physics, *Meteorol. Monogr.*, in press, 2002.

Rutledge, S. A., E. R. Williams, and T. D. Keenan, The Down Under Doppler and Electricity Experiment (DUNDEE): Overview and preliminary results, *Bull. Am. Meteorol. Soc.*, *73*, 3–16, 1992.

Sagalyn, R. C., The production and removal of small ions and charged nuclei over the Atlantic Ocean, in *Recent Advances in Atmospheric Electricity*, edited by L. G. Smith, Pergamon, New York, 1958.

Sagalyn, R. C., and G. A. Faucher, Aircraft investigation of the large ion content and conductivity of the atmosphere and their relation to meteorological factors, *J. Atmos. Terr. Phys.*, *5*, 253–272, 1954.

Satori, G., and B. Zieger, Spectral characteristics of Schumann resonances observed in Central Europe, *J. Geophys. Res.*, *101*, 29,663–29,670, 1996.

Saunders, C. P. R., W. D. Keith, and R. P. Mitzeva, The effect of liquid water on thunderstorm charging, *J. Geophys. Res.*, *96*, 11,007–11,017, 1991.

Scerne, R. M. S., A. O. Santos, M. M. dos Santos, and F. A. Neto, Aspectos agroclimaticos da regiao do Ouro Preto d'Oeste-Rondônia, *Bol. Tec. 13*, Minist. da Agric. e do Abastecimento, CEPLAC, Superintendencia Reg. da Amazonia Oriental, Belém, Pará, Brazil, 1996.

Squires, P., The microstructure and colloidal stability of warm clouds, *Tellus*, *10*, 256–271, 1958.

Takahashi, T., Riming electrification as a charge generation mechanism in thunderclouds, *J. Atmos. Sci.*, *35*, 1536–1548, 1978.

Watkins, N. W., M. A. Clilverd, A. J. Smith, C. J. Rodger, N. A. Bharmal, and K. H. Yearby, Lightning atmospherics count rates observed at Halley, Antarctica, *J. Atmos. Terr. Phys.*, *63*, 993–1003, 2001.

Whipple, F. J. W., On the association of the diurnal variation of electric potential gradient in fine weather with the distribution of thunderstorms over the globe, *Q. J. R. Meteorol. Soc.*, *55*, 1–17, 1929.

Williams, E. R., The Schumann resonance: A global tropical thermometer, *Science*, *256*, 1184–1187, 1992.

Williams, E. R., Global circuit response to seasonal variations in global surface air temperature, *Mon. Weather Rev.*, *172*, 1917–1929, 1994.

Williams, E. R., Global circuit response to temperature on distinct time scales: A status report, in *Atmospheric and Ionospheric Electromagnetic Phenomena Associated With Earthquakes*, edited by M. Hayakawa, Terra Sci., Tokyo, 1999.

Williams, E. R., and S. J. Heckman, The local diurnal variation of cloud electrification and the global diurnal variation of negative charge on the Earth, *J. Geophys. Res.*, *98*, 5221–5234, 1993.

Williams, E. R., and N. O. Renno, An analysis of the conditional instability in the tropical atmosphere, *Mon. Weather Rev.*, *121*, 21–36, 1993.

Williams, E. R., S. A. Rutledge, S. G. Geotis, N. Renno, E. Rasmussen, and T. Rickenbach, A radar and electrical study of tropical "hot towers", *J. Atmos. Sci.*, *49*, 1386–1395, 1992.

World Meteorological Organization, World distribution of thunderstorm days, parts I and II, *WMO Publ. 21*, Geneva, 1956.

Zipser, E. J., Deep cumulonimbus cloud systems in the tropics with and without lightning, *Mon. Weather. Rev.*, *122*, 1837–1851, 1994.

Zipser, E. J., Some views on "hot towers" after 50 years of tropical field programs and two years of TRMM data, *Meteorol. Monogr.*, in press, 2002.

Zipser, E. J., and M. A. LeMone, Cumulonimbus vertical velocity events in GATE, part II, Synthesis and model core structure, *J. Atmos. Sci.*, *37*, 2458–2469, 1980.

Zipser, E. J., and K. Lutz, The vertical profile of radar reflectivity of convective cells: A strong indicator of storm intensity and lightning probability, *Mon. Weather. Rev.*, *122*, 1751–1759, 1994.

---

M. Antonio, B. Biazon, R. Camargo, H. Franca, A. Gomes, M. Lima, R. Machado, S. Manhaes, L. Nachtigall, H. Piva, and W. Quintiliano, Instituto de Pesquisas Meterologicas, Avenida Luiz Edmundo Carrijo Coube S/No, CEP 17033-360 Bauru/SP, Brazil. (Mauricio@www.radar.ipmet.unesp.br)

P. Artaxo, Universidade Sao Paulo, Instituto de Fisica, CAIXA Posatal 66-318, CEP 05389-970, SP, Brazil. (Artaxo@if.usp.br)

E. Avelino, EMBRATEL, Porto Velho, Rondinia, Brazil. (e.avelino@uol.com.br)

A. Betts, Atmospherica Research, 58 Hendee Lane, Pittsford, VT, 05763, USA. (Akbetts@aol.com)

R. Blakeslee, J. Bailey, and D. Bocippio, NSSTC, NASA/MSFC, 320 Sparkman Dr., Huntsville, AL 35805, USA. (Rich.Blakeslee@msfc.nasa.gov; Jeff.bailey@msfc.nasa.gov; Dennis.boccippio@msfc.nasa.gov)

J. Fuentes, University of Virginia, Charlottesville, VA, USA. (jf6s@unix.mail.virginia.edu)

J. Gerlach, N. Gears, L. Atkinson, N. Dunnemann, and G. Frostrom, Wallops Island Flight Facility, NASA Goddard Space Flight Center, Wallops Island, VA 23337-5099, USA. (John.C.Gerlach.1@gsfc.nasa.gov)

L. Machado, Centro Tecnico Aerospacial, Divisao de Ciencias Atmosfericas, Sao Jose dos Campos 12228-904, Sao Paolo, Brazil. (Machado@iae.cta.br)

N. Madden, 5 Willard Circle, Bedford, MA, 01730, USA. (ntmadden@yahoo.com)

N. Renno, Atmospheric Sciences, University of Arizona, Tucson, AZ 85721, USA. (Renno@soar.atmo.arizona.edu)

G. Roberts, Scripps Institue of Oceanography, 9500 Gilman Dr. 0239, La Jolla, CA 92093, USA. (greg@fiji.ucsd.edu)

E. Williams, Parsons Laboratory, MIT 48-211, Cambridge, MA 02139, USA. (Earlew@ll.mit.edu)

D. Wolff, B. Roy, J. Halverson, and T. Rickenbach, Laboratory for Atmospheres, NASA Goddard Space Flight Center, Greenbelt, MD 20771, USA. (Halverson@agnes.gsfc.nasa.gov; Ricken@trmm.gsfc.nasa.gov)